LJMU Research Online

Mirkhalafi, S, Hashim, KS, Al-Hashimi, O and Majdi, A

 Hybrid Electrocoagulation–Adsorption Process for Montelukast Sodium Removal from Water

http://researchonline.ljmu.ac.uk/id/eprint/24868/

Article

For more information please contact researchonline@ljmu.ac.uk

Article

Hybrid Electrocoagulation–Adsorption Process for Montelukast Sodium Removal from Water

Sayedali Mirkhalafi [1,*], Khalid S. Hashim [1,*], Osamah Al-Hashimi [1] and Ali Majdi [2]

[1] Faculty of Engineering and Technology, School of Civil Engineering and Built Environment, Liverpool John Moores University (LJMU), Liverpool L3 3AF, UK; o.a.alhashimi@2020.ljmu.ac.uk
[2] Department of Buildings and Construction Techniques Engineering, College of Engineering, Al-Mustaqbal University, Hillah 51001, Iraq
[*] Correspondence: s.mirkhalafi@2024.ljmu.ac.uk (S.M.); k.s.hashim@ljmu.ac.uk (K.S.H.)

Abstract: This study addresses the significant environmental challenge of pharmaceutical pollutants by demonstrating the effectiveness of a hybrid electrocoagulation–adsorption (EC-A) technique for removing Montelukast Sodium (MS) from contaminated water. The research was conducted in three stages—adsorption, electrocoagulation, and adsorption using the residual water from the electrocoagulation process. The adsorbent materials were characterised using various analytical techniques: X-ray Diffraction (XRD) for determining the crystalline structure, Energy-Dispersive X-ray Spectroscopy (EDX) for elemental composition, Scanning Electron Microscopy (SEM) for surface morphology, and Fourier Transform Infrared Spectroscopy (FTIR) for identifying functional groups before and after interaction with the pollutants. The adsorption phase achieved optimal results at a pH of 3 and a contact time of 120 min, with a maximum removal efficiency of 99.5% for a starting MS concentration of 50 mg/L using Calcium Ferric Oxide–Silica Sand (CFO-SS) adsorbent. The electrocoagulation phase showed a 97% removal efficiency with a pH of 11, a current density of 20 mA, and a 5 mm electrode distance, achieved in just 20 min. Finally, the combined EC-A process, with the pH of residual water adjusted to 3, further enhanced the removal efficiency to 74%, highlighting the method's potential for pharmaceutical contaminant removal. These findings underscore the potential of the EC-A technique as a highly effective and adaptable solution for mitigating pharmaceutical contaminants in water.

Keywords: electrocoagulation; adsorption; hybrid EC-A treatment; montelukast sodium; water treatment

1. Introduction

A UN report from the 2023 Water Conference reveals that 2 billion people lack safe drinking water, and 3.6 billion lack proper sanitation, highlighting a global crisis. The government of the UK has also raised concerns about a future water crisis, emphasising the need for effective water treatment. Contaminants in water bodies are a major environmental threat, accumulating in ecosystems and posing risks to human health and wildlife [1]. The report stresses the urgent need for improved water and wastewater treatment to protect both current and future generations. Pharmaceuticals are one of the common contaminants found in wastewater and surface waters, and they can cause serious issues. Previous works indicate that even at low concentrations, these organic pollutants can cause serious issues [2,3]. These compounds have been found in large amounts in drinking water, sewage, sediment, surface water, and aquaculture effluent [4,5]. Pharmaceuticals can reach the aquatic environment via a variety of sources, such as the outflow of home sewage, medical facilities, and some types of industrial wastewater [6]. Because of this, there is currently a serious environmental issue due to the extensive use of pharmaceuticals and environmental degradation. Consequently, there is increasing interest in removing drugs from natural water sources [7]. However, the treatment of pharmaceutical wastewater might be difficult

thanks to its complex and variable nature, which makes conventional methods difficult to employ [8].

Several methods have been employed for removing pollutants, particularly pharmaceuticals from water, including reverse osmosis (RO) [9], photocatalysis [10], ion exchange [11], biological processes [12], adsorption [13], electrocoagulation (EC) [14–16], and electrocoagulation–adsorption (EC-A) [8]. Each method has advantages and drawbacks, and the reasons EC-A was employed for this study are the energy efficiency, reduced chemical usage, ease of operation, and cost-effectiveness of the EC-A method.

Employing electrical currents that degrade and separate contaminants from wastewater, electrocoagulation (EC) is an advanced water treatment technique that provides an effective and sustainable solution for a range of purification requirements. In reference to earlier research on the removal of pharmaceuticals by electrocoagulation (EC), a study successfully demonstrated the removal of cefazolin (CEZ) from pharmaceutical wastewater utilising iron electrodes in EC, obtaining a noteworthy removal efficiency of 85.65% [17]. Nariyan et al. investigated the use of electrocoagulation with different anode–cathode configurations to remove oxytetracycline hydrochloride. When comparing the anode materials of iron and aluminium, they discovered that the latter was more efficient. For both anodes, 20 mA/cm^2 was the ideal current density, resulting in removal efficiencies of 87.75% for aluminium and 93.2% for iron [18]. Ensano et al.'s subsequent investigation proved that electrocoagulation worked well for treating ordinary municipal wastewater that had been tainted with drugs. Drugs like amoxicillin, carbamazepine, and diclofenac showed remarkable clearance efficiencies ranging from 70% to 90%. Their examination of additional pollutants, including chemicals, organic compounds, and UV-absorbing materials, also revealed that longer process times and higher electrical inputs resulted in a higher level of pollution removal. They discovered that using a certain quantity of electricity and letting the process run for about 19 h produced the best results [19]. Another study employed aluminium electrodes for the cathode and anode in electrocoagulation (EC) to extract acetaminophen (paracetamol) from river water. This strategy revealed an operational cost of USD 0.22 per cubic metre for EC-based river water treatment, and it produced good outcomes [20]. All the investigated studies have illustrated the efficiency of electrocoagulation for the removal of pharmaceutical pollutants from contaminated water and wastewater.

Adsorption is a highly efficient process employed for water treatment that removes pollutants, including heavy metals, organic compounds, and pathogens, from water by collecting and retaining them on the surface of solid materials, and several studies have investigated the removal efficiency of adsorption in pharmaceutical removals. Using a co-precipitation method, Yegane Badi et al. created powder-activated carbon modified with magnetite nanoparticles or PAC-MNPs. The purpose of this modified carbon was to adsorptive remove Ceftriaxone from aqueous solutions. It was discovered that PAC-MNPs have a 97.18% Ceftriaxone adsorption capability. The results of the investigation showed that polygonal Fe_3O_4 nanoparticles were evenly dispersed across the PAC surface, with diameters less than 75–100 nm. PAC-MNPs' upper surface was covered in uniformly spaced, unevenly shaped gaps of different sizes. It was determined that these surface imperfections served as the main locations for Ceftriaxone adsorption [21]. Activated carbon was employed as the adsorbent in a study that examined the adsorption-based removal of Tetracycline (TC) and Lincomycin (LM) from water, with a removal efficiency of 95% [22]. Another study used a green synthesis of silver-reduced graphene (Ag-RGO) at 24.25 °C and 20.2 mg of adsorbent to extract Naproxen (NPX) from water with 92.62% efficiency [23].

Increasingly, researchers are focusing on the integrated electrocoagulation-assisted adsorption (ECA) system with solar photovoltaic power supply as a successful method of reducing chemical oxygen demand (COD) from pharmaceutical effluent. Numerous operational factors, such as electrode number, configuration, distance, operating time, current density, adsorption time, and temperature, were examined in a recent study that used the

EC-A approach. The largest COD reductions were obtained with an MP-P configuration, six electrodes, a current density of 6.656 mA/cm^2, a temperature of 45 °C, a time of 20 min, a distance of 4 cm, and an MP-P configuration. The operating cost of conventional energy was 0.273 USD/m3. Efficient COD reductions of 85.4, 69.1, and 95.5% were attained by the EC, adsorption, and combination of EC and adsorption procedures, respectively [8].

In this current study, a hybrid EC-A approach has been investigated for the removal of Montelukast Sodium (MS) from synthetic water. Despite the lack of previous works on MS removal from water, a study by Siciliano et al. has shown the presence of MS in the environment and warns about the toxicity of this drug that can put both humans and animals in danger [24]; this current work aims to remove this chemical pollutant for the first time using a hybrid EC-A approach. The removal efficiency has been investigated in three different stages: adsorption (continuous batch experiments), EC tests, and adsorption after EC with the residual contaminated water. The novel engineered sand activated with calcium ferric oxide named CFO-SS (Calcium Ferric Oxide–Silica Sand), which was manufactured by the authors and tested successfully for Tetracycline (TC) removal [25], has been used in this study as an adsorbent.

2. Materials and Methods

2.1. Chemicals and Instruments

Wastepaper sludge ash, which was supplied from Saica Paper Ltd, Partington, Manchester, UK., has been used with the physical conditions of a pH of 12.31, 13.34 μm mean diameter, bulk density of 561 kg/m3, and SG of 2.5. Furthermore, industrial sand was supplied by LJMU with a mean diameter of 1013 μm, SG of 2.685, hydraulic conductivity of 4.719×10^{-1} cm/s, and a porosity of 0.37, and also supplied FeCl$_3$ (with the purity of 97%), HCL (32%), NaOH, and ethylene glycol (with the purity of 99%). Besides the mentioned material, Montelukast Sodium (MS), with the chemical formula of C$_{35}$H$_{36}$ClNO$_3$S (Figure 1), with a molecular weight of 608.17 g/mol, and Sodium Chloride (NaCl, purity > 99%), with a molecular weight of 58.44 g/mol, were supplied from Merck, UK.
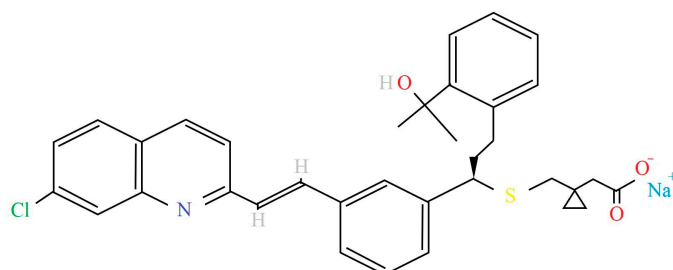
Figure 1. Montelukast Sodium (MS) chemical structure.

2.2. Preparation of Adsorbent

The process of remanufacturing the activated sand is used based on the authors' previous studies [25,26]. A total of 100 mL of DI water containing 1.5 mL of HCl (32%) was mixed with two grammes of wastewater sludge ash and stirred at the speed of 200 rpm at room temperature for 180 min. Then, the solution was filtered via Whatman filter paper grade (1) at a diameter of 90 mm to collect calcium ions (Ca^{2+}) dissolved in the clear filter solution, and the pH of this solution was adjusted to 12 using NaOH. Subsequently, a precisely measured 3.66 g of FeCl$_3$ was added to the solution to attain a molar ratio of 1:0.75 between Ca^{2+} and FeCl$_3$. A total of 3.66 g of quartz sand was added to the mixture, yielding a dose of 1 Sand: 1 FeCl$_3$. A glass flask containing an appropriate volume (6 mL) of ethylene glycol was decanted and agitated at 200 rpm for three hours to create a layer of calcium ferric oxides on the sand's surface. The mixture was then filtered to remove the sand and solution using the Whatman filter paper grade (1). After that, the resulting sand was dried for 12 h at 95 °C in an air-ventilated oven. The sand was then stored in a dry and clean glass bottle at room temperature for later use in batch tests. The

experimental setup process is shown in Figure 2 below. As shown in the flowchart, the first step is manufacturing the adsorbent (CFO-SS); then, the first stage of the experiment is the adsorption batch experiment with the best conditions, the second is electrocoagulation with the best conditions, the third stage is the adsorption batch test with the residual water of the second stage, and finally, characterizations are performed for the adsorbent of the first and third stage and compared with the raw and activated sand.
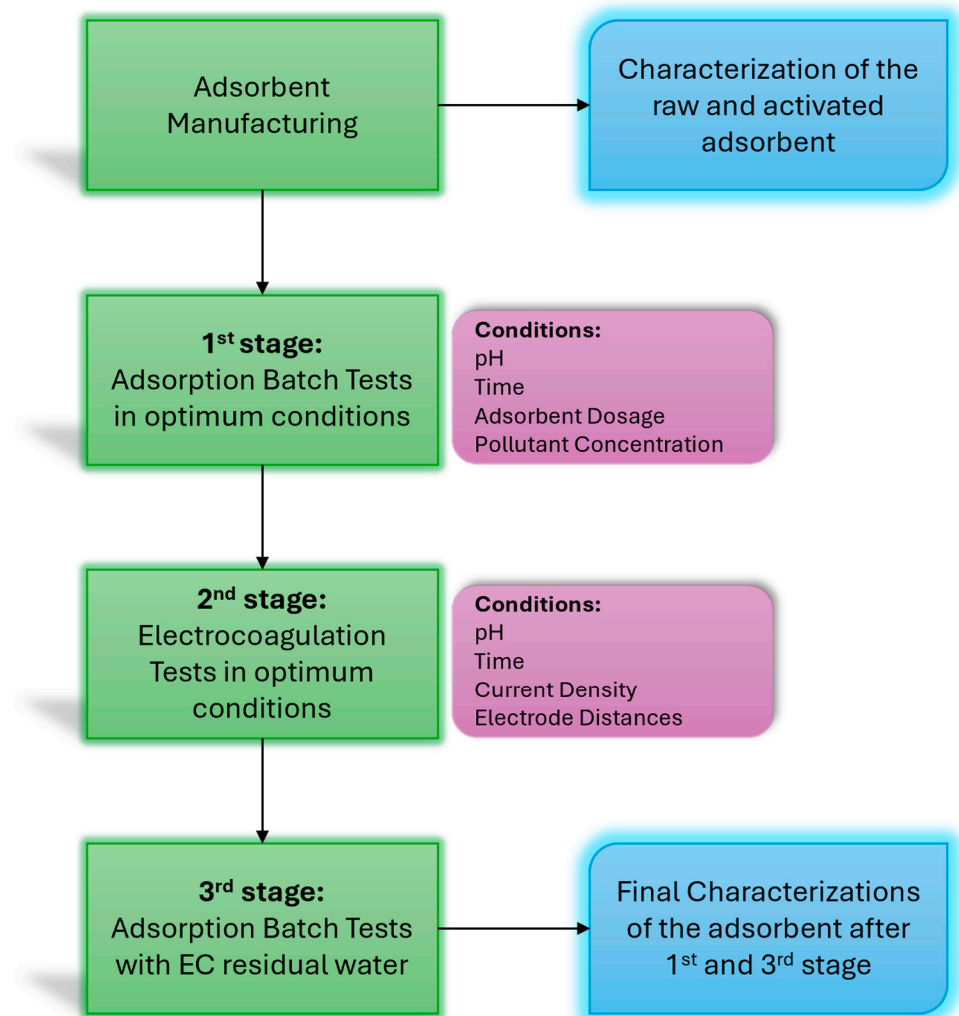
Figure 2. Experimental setup for hybrid electrocoagulation–adsorption (EC-A) experiment.

2.3. Adsorption Batch Tests

Using a series of batch experiments under varying settings, the effectiveness of activated sand was examined in the first stage of the experiments for the removal of Montelukast Sodium from water, based on the technique previously employed by [27,28].

The concentration of MS was measured both before and after the removal using a tabletop Visible Spectrophotometer (UV-Spectrophotometer) type HACH-lang DR3900, manufactured by Hach Lange GmbH Headquarter (Düsseldorf, Germany). Additionally, the peak absorbance for each of the three random MS doses has been measured to determine the wavelength, which is found at $\lambda_{max} = 355$ nm.

Furthermore, utilising a range of MS concentrations (25–150 mg/L), a calibration curve for MS readings was produced. This curve was created and computed using Microsoft Excel 365. Then, sets of 250 mL glass flasks, each holding 100 mL of DI water (17.5 MΩ), were used in the batch studies. To guarantee appropriate interaction between the pollutant (MS) and the activated sand, 0.05 g of CFO-SS was applied to each flask and subsequently shaken

using a tabletop CORNING-LSE shaking incubator. Whatman filter paper grade 5 was used to filter out the suspended reactive media particles, yielding a clear solution of the treated water after 180 min of shaking.

The batch investigations aimed to find the ideal operating conditions for the best possible adsorption. These investigations looked at the effects of varying starting MS concentrations (25–150 mg/L) throughout time (10–180 min), pH (3–12), and CFO-SS doses (0.05–0.5 g). Subsequently, the produced materials after their contact with MS, CFO-SS, and raw silica sand were analysed using Fourier transform infrared analysis (FT-IR), Scanning Electron Microscopy (SEM), Energy-Dispersive X-ray (EDX) and X-ray Diffraction (XRD) techniques.

2.4. Calibration Curve

Initial concentrations (25, 50, 75, 100, 125, 150 mg/L) of Montelukast Sodium were contacted with 0.05 g of adsorbent (CFO-SS) and measured with the UV–vis spectrophotometer, and then the calibration curve was established using Microsoft Excel; the value of R^2 was calculated for finding the removal efficiency of each experiment. The data reported in Figure 3 were fitted by a curve line, and the correlation coefficient at the highest level was found (R^2 = 0.924). The high correlation coefficient of the calibration line observed in this study indicates that the absorptivity is consistent across the concentration range analysed, ensuring that the MS concentration can be determined with high precision [29].
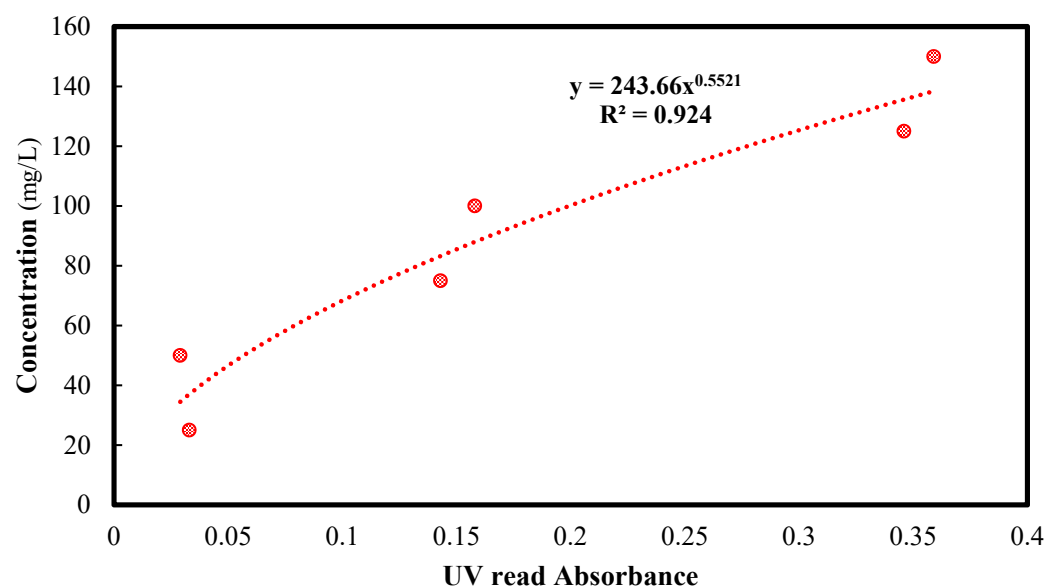
Figure 3. Calibration curve diagram and R^2 value for MS concentrations.

2.5. Operational Conditions

The batch tests examined the appropriate operating parameters, which include the starting pH, the absorbent dosage, the impact of contact duration, and the beginning MS concentration (C_0). In all tests, 250 mL glass flasks, each holding 100 mL of contaminated water with various MS concentrations (25, 50, 75, 100, 125, 150 mg/L) were examined; 0.05 g of the activated sand was used in each glass flask, and the agitation speed was constant at 200 rpm. After 10, 20, 30, 60, 120, and 180 min, the water was filtered with paper filters and measured with a UV spectrophotometer. The volume of pollutant on the adsorbent (q_e) and the quantity of MS stored in the adsorbent (q_e, mg/g) were calculated using Equation (1), which is based on the mass balance principle.

$$q_e = (C_0 - C_e)\frac{V}{m} \tag{1}$$

where V is the volume of the aqueous solution (L), m is the mass of the adsorbent (g), C_0 and C_e are the initial and final concentrations of MS (mg/L), respectively, and q_e is the volume of adsorbate placed on the adsorbent (mg/g). Equation (2) was used to discover the removal efficiency (R%) of MS.

$$R(\%) = \frac{(C_0 - C_e)}{C_0} \times 100 \qquad (2)$$

2.6. Adsorption Isotherm

To maximise efficiency in the study of adsorption-based water treatment, it is essential to comprehend the mechanisms governing the adsorption process. Adsorption isotherms, which show the relationship between the amount adsorbed onto the adsorbent at equilibrium and the concentration of adsorbate in solution, are examined in this process. In this current study, Freundlich and Langmuir isotherms were calculated using Equations (3) and (4).

Freundlich Isotherm: An empirical model used to represent adsorption on heterogeneous surfaces is the Freundlich isotherm. Here is how Equation (3) represents it:

$$q_e = K_f C_e^{1/n} \qquad (3)$$

where q_e is the amount of adsorbate adsorbed per unit mass of adsorbent at equilibrium (mg/g), C_e is the equilibrium concentration of the adsorbate in the solution (mg/L), K_f is the Freundlich constant indicative of adsorption capacity, and *n* is a constant related to the intensity of adsorption.

Langmuir Isotherm: If adsorption takes place in a monolayer, the Langmuir isotherm is a theoretical model that represents adsorption on homogeneous surfaces with finite identical sites. The following is the Langmuir equation (Equation (4)):

$$q_e = \frac{q_{max} K_L C_e}{1 + K_L C_e} \qquad (4)$$

where q_e is the amount of adsorbate adsorbed per unit mass of adsorbent at equilibrium (mg/g), q_{max} is the maximum adsorption capacity of the adsorbent (mg/g), K_L is the Langmuir constant related to the affinity of binding sites (L/mg), and C_e is the equilibrium concentration of the adsorbate in the solution (mg/L).

2.7. Adsorption Kinetic

Adsorption kinetics also shed light on the dynamics of solute uptake over time by revealing the rate at which adsorption takes place. In this paper, the Pseudo-First and -Second-Order models were investigated using Equations (5) and (6) as shown below:

Pseudo First Order: The following equation represents the Pseudo-First-Order model [30].

$$q_t = q_e \left(1 - e^{-k_1 t}\right) \qquad (5)$$

where k_1 is the Pseudo-First-Order rate of adsorption (min^{-1}), q_e represents the amount of pollutant adsorbed by the reactive media in the equilibrium conditions (mg/g), and q_t is the quantity of the pollutant adsorbed at a specific time (t) (mg/g).

Pseudo Second Order: The following equation could be used to quantify the Pseudo Second Order [31].

$$q_t = \frac{t}{\left(\frac{1}{1/K_2 q_e^2} + \frac{t}{t/q_t}\right)} \qquad (6)$$

where k_2 is the Second-Order sorption's rate constant (mg/(mg.min)). At extremely low initial concentrations, the sorption rate might be determined using the Pseudo-Second-Order adsorption kinetic model.

2.8. Electrocoagulation (EC) Tests

In the second phase, EC was carried out separately to measure the removal of efficiency of MS, with the optimum concentration after batch experiments (50 mg/L), with various parameters such as pH, time, current density (CD), and distance between electrodes; then, the optimised condition was investigated. The set of EC experiment machines contains a DC power supply manufactured by British Standard Tester (BTS 2/5A, two Channel Regulated), a bench-scale reactor with a capacity of 1.2 L, and a peristaltic pump manufactured by Watson Marlow (504 U). Also, the electrodes used in this study were made from aluminium, with a dimension of 110×55 mm, and washed with HCL and rubbed with sand filters prior to each experiment to prevent cross-contamination and restore the surface activity of electrodes.

To run the experiment, a one-litre beaker containing DI water was filled, stirred, and mixed with 50 mg per litre of MS. The mixture was then drained into the reactor to investigate the removal efficiency under a range of conditions, including pH (3–11), time (10–60 min), distance between electrodes (5–15 mm), and current density (10–30 mA). The solution's pH was adjusted to be less than and higher than neutral by adding HCL and NaOH, respectively.

The experiment started by examining the pH effect. Using the same UV Spectrophotometer, the solution in the reactor was measured after 5, 10, 15, and 20 min, with the pH starting at 3 and going up to 11. This allowed researchers to determine the ideal pH. The best pH was then used in the experiments to investigate the ideal distance between the electrodes. Following the determination of the ideal distance, pH, and electrode spacing, the impact of current density (CD) was studied at 10, 20, and 30 mA, leading to the identification of the optimal CD. Finally, at the final experiment in this phase, different contact times in 10, 20, 30, 40, 50, and 60 min were measured, and ultimately the ideal conditions were looked at.

2.9. Batch Test for EC Residual Water

After determining the ideal conditions, the adsorption batch experiment for the leftover water was carried out as the last phase of the hybrid EC-A experiment. This was achieved after an hour of contact with the electrodes. Subsequently, water aluminium from the electrode was mixed with different dosages of CFO-SS in the same shaking incubator under ideal conditions realised during the adsorption batch experiments. At the end of the experiment, the removal efficiency of the contaminated water was assessed using a UV Spectrophotometer. Since the optimal condition of adsorption during the first stage was in the acidic phase and the optimal condition during the second phase was in the alkalinity phase, acidification was carried out prior to the last phase. This was carried out using HCL to lower the pH of the residual water after EC from 11 to 3.

3. Results and Discussion

In this section, the results of adsorption (the experiment's first stage), electrocoagulation (the experiment's second stage), and adsorption with the EC residual water (the experiment's third stage) have been provided. The experimental design as mentioned above is in the best condition for the previous part. It means that for instance after evaluating the effect of adsorbent dosage, the next stage which is the effect of pH has been conducted with the best adsorption dosage in the previous section, and this method was followed constantly during all the experiments in this research and explained in detail in each subsection.

3.1. Sorption Batch Tests

Montelukast Sodium ($C_{35}H_{36}ClNO_3S$) is mostly adsorbed onto silica sand activated with calcium ferric oxide ($CaFe_2O_4$) by hydrogen bonding [32], van der Waals forces [33], and electrostatic interactions [34]. In addition to adding reactive sites and increasing surface area, the activated silica sand also adds positive charges that draw in the negatively charged

montelukast. To facilitate the adsorption process, montelukast's functional groups, such as carboxylic and amine groups, can create hydrogen bonds with the silica surface's hydroxyl groups. This interaction is as simple as the solid adsorbent reacting with montelukast in solution, which causes the montelukast to be adsorbed onto the activated silica sand's surface. Temperature, initial concentration, adsorbent dosage, pH, and contact time all have a major impact on the adsorption process's overall effectiveness.

For this purpose, a series of batch adsorption experiments were conducted under different conditions, such as pH, time, and adsorbent dosage, for different concentrations of the adsorbent. The removal efficiency measured for the pH of 3, 7, and 11, contact time after 10, 20, 30, 60, 120, and 180 min, adsorbent dosage at 0.05, 0.1, 0.2, 0.3, 0.4 and 0.5 g, and the initial concentration (C_0) of MS at 25, 50, 75, 100, 125, and 150 mg/L were also used for the developing a calibration curve. Every experiment was run three times to validate the findings of the current work, and the results displayed in the figures are the average of those three runs.

For concentrations of 25, 50, 75, 100, 125, and 150 mg/L, the amount of time needed to reach the equilibrium state was studied. The conditions for the conduction of the batch experiment were a pH of 7, activated sand dosage of 0.05 g for 100 mL of polluted water with MS, and agitation speed of 200 rpm at room temperature.

According to the results, the best removal efficiency was reached after 120 min of contact between the adsorbent and pollutant, because after that the removal efficiency stayed steady in each concentration, which means that the capacity of 0.05 g of activated sand became full. No huge changes were visible in the results between 2 and 3 h of contact between activated sand and contaminations. The best removal efficiency in all concentrations was achieved in 50 mg/L with an efficiency of 45.4% that shows over 50% of MS remained in the water in the best condition. The lowest removal efficiency was also found after 10 min with the initial concentrations of 75 mg/L, with a percentage of 6.5%. The batch experiment continued to discover the highest removal efficiency of MS and the best condition for reaching the best removal. Therefore, the effect of adsorbent dosage with the same pH and the performance of the adsorbent in acidic and alkaline phases were investigated, and the performance of the adsorbent in each stage was discovered.

3.1.1. Effect of Adsorbent Dosage

The best removal efficiency in the previous section was found in the initial concentration of 50 mg/L with a percentage of 45.4% after 120 min of connection time. In this section of the experiment, the effect of adsorbent dosage was investigated. The batch experiments were conducted with an initial concentration of 50 mg/L, pH of 7, and 2 h of contact time. The dosages of adsorbent utilised were 0.05, 0.1, 0.2, 0.3, 0.4, and 0.5 g of activated sand (CFO-SS) in the mentioned condition. The result is shown in Figure 4; as the dosage of adsorbent increased, the efficiency of removal improved in a logical order. The highest removal efficiency was found at 60% after 120 min of contact with 0.5 g of adsorbent, while it was around 45% with a dosage of 0.05 g. Although 60% of removal was achieved with 0.5 g of adsorbent, the experiments continued to determine the performance of activated sand at different pH levels.

Compared to the previous studies, it can be concluded that the effect of adsorbent dosage could affect the adsorption capacity. In one study for the removal of chromium (Cr) from synthesised wastewater, removal efficiency improves first, reaches its maximum, and subsequently declines as adsorbent dosage increases while keeping all other parameters at fixed values; in this current study, the removal efficiency increased steadily with the increase in the adsorbent dosage [35]. In another study for the removal of Pb and Cd from the water, it was investigated that by increasing the adsorbent dose, the removal efficiency increased from around 75 to 90%, which showed the same increase as this current study [36]. In this study, the adsorbent performed better at higher dosages because more adsorption sites were available, enhancing the chances of capturing and removing the adsorbate from the solution.
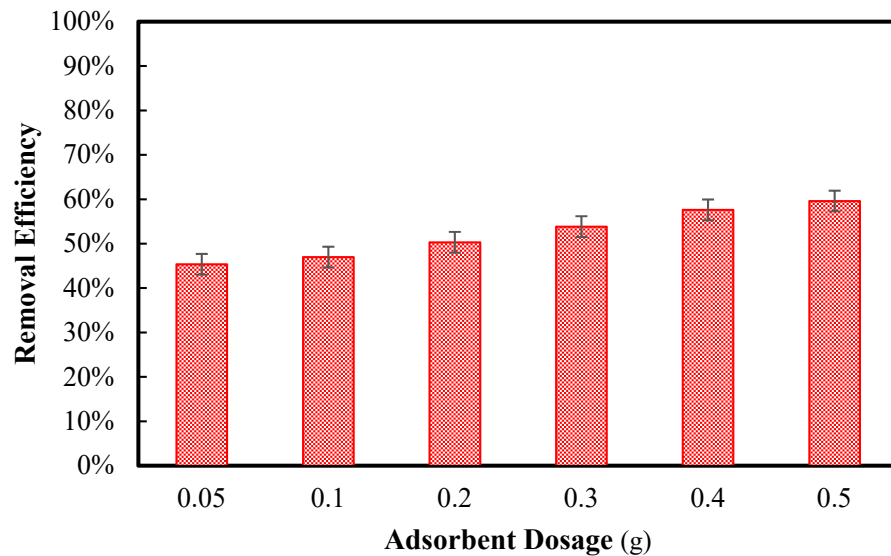
Figure 4. Effect of adsorbent dosage on MS removal.

3.1.2. Effect of pH

With the initial concentration of 50 mg/L and the same adsorbent dosage as the initial batch experiments, which was 0.05 g, and the best removal time, which was found at 120 min, the effect of pH was investigated. Three batch experiments were conducted with a pH of 3, pH of 7, and pH of 11 to determine the performance of the adsorbent in the acidic, neutral, and alkaline phases. Each experiment was conducted three times, and the validity of the results was approved. The result of the experiments is shown in Figure 5. Based on the results, the best performance of the adsorbent was found at a pH of 3, with a removal efficiency of 84%, which shows that the adsorbent is very efficient in the acidic phase.
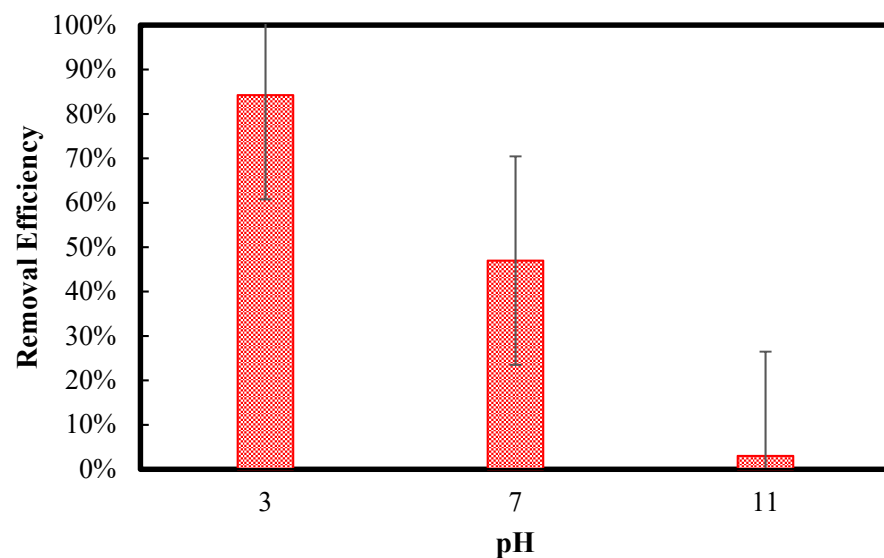
Figure 5. Effect of pH on the performance of adsorbent on MS removal.

In the previous study conducted by the authors, however, the best pH was found around 10 for the removal of Tetracycline from the water with the same adsorbent [26]. The same result has been investigated in another study for the removal of chromium ions from industrial effluent using activated carbon as the adsorbent. The best pH in this study was also found to be around 10, and after that value, the efficiency of work tends to decrease [37]. On the other hand, in the study for the removal of hexavalent chromium from wastewater, the best pH was found to be around 3, the same as this current work [35]. The reason

that the adsorbent in this study performs better at pH 3 is that the surface charge of the adsorbent becomes more positive, enhancing electrostatic attraction to negatively charged species while preventing precipitation and ensuring optimal ionisation of the adsorbate.

3.1.3. Optimum Conditions and Best Removal Efficiency of MS

After the best pH was found to be 3 and the time was found to be 120 min, the experiments continued to reach the highest removal efficiency of MS. The tests were carried out with the initial concentration of 50 mg/L and activated sand dosages of 0.05, 0.1, and 0.15 g, and repeated three times. The results are shown in Figure 6, and the best removal efficiency of Montelukast Sodium (MS) from contaminated water with the initial concentration of 50 mg/L, 0.1 g dosage of CFO-SS as adsorbent, 120 min of contact time, and pH of 3 was achieved with the rate of 99.5% removal.
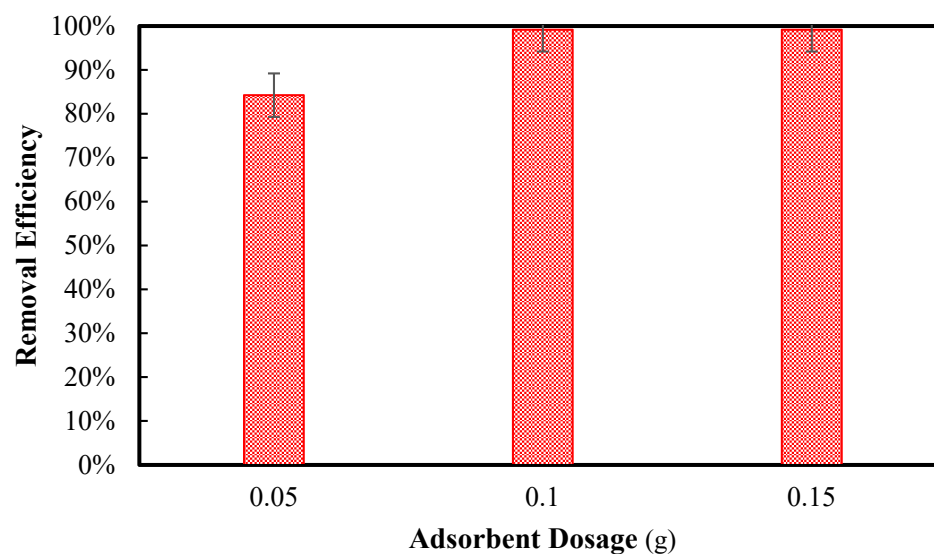

Figure 6. Best removal efficiency of MS from water.

3.2. Hybrid Electrocoagulation–Adsorption (EC-A) Tests

3.2.1. Electrocoagulation

To remove Montelukast Sodium ($C_{35}H_{36}ClNO_3S$) from water, the electrocoagulation (EC) method employing aluminium electrodes involves the following crucial steps. Hydroxide ions (OH^-) are produced when aluminium is reduced at the cathode, whereas aluminium ions (Al^{3+}) are released into the solution when aluminium is oxidised at the anode [38]. After that, the aluminium ions combine with hydroxide ions to create aluminium hydroxide ($Al(OH)_3$), a coagulant. By forming micro-flocs through electrostatic attraction and hydrophobic interactions, these coagulants efficiently absorb montelukast. It will be easier to remove montelukast from the water if the flocs that develop settle due to gravity. Important variables affecting this process include electrode distance, which affects the electric field strength and current efficiency; contact time, which is essential for efficient adsorption and removal; pH, which affects the solubility of aluminium hydroxide; and current density, which affects the rate of coagulant generation.

After conducting the batch experiments for MS removal from polluted water, electrocoagulation experiments were conducted in the second phase of the study to evaluate the efficiency of these experiments for MS removal from water. The effect of pH, the distance between electrodes (mm), current density (mA), and time (min) have been investigated before the conduction of the third phase of the experiment, which is adsorption with the residual water after the electrocoagulation test. A hybrid electrocoagulation–adsorption experiment was conducted after the best conditions were found. The experiment was started with the effect of pH, and after the best pH was found, another test set was conducted to find out the effect of distance between electrodes on the removal efficiency of

MS. The initial concentration of MS in the pollutant was investigated from the adsorption test, which was found to be 50 mg/L. With the best pH and electrode distance, the effect of current density has been investigated and with the best conditions (pH, electrode distance, and current density), the effect of time was evaluated, and the best removal efficiency was found to be 100% of MS removal from contaminated water under pH 11, 5 mm electrode distances, current density of 20 mA, and after 20 min contact with electrodes. To validate the results of this current study, all the experiments were conducted three times, and the results shown in the figures are averages of three tests.

Effect of pH

The electrocoagulation tests started with the effect of pH. For this purpose, a set of EC experiments were conducted in a pH of 3, 7, and 11. The initial pollutant concentration was 50 mg/L, and the distance between electrodes was adjusted to 5 mm. After 5, 10, 15, and 20 min, samples were taken out from the reactor, filtered with paper filter number 5, and measured with the spectrophotometer, and the results for the removal are shown in Figure 7.
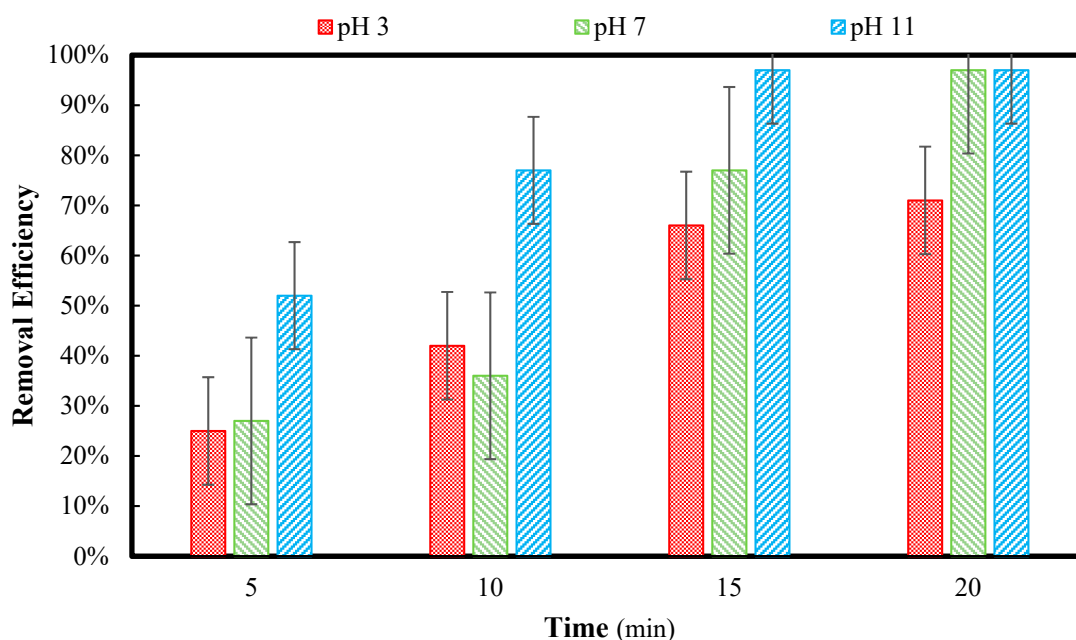

Figure 7. Effect of pH on EC test in pH 3, 7, and 11 after 5, 10, 15, and 20 min of the test.

Results have shown the efficiency of electrocoagulation in different phases (acidic, neutral, alkaline). The best performance was found in pH 11, where 97% removal efficiency was reached after 15 min, while in pH 3, the best removal efficiency was 71% after 20 min of the experiment. In pH 7, also, the highest removal efficiency was found after 20 min of contact time, which was found at 97%, as well as pH 11, but in more time. Therefore, the other tests would have been conducted with the best pH, which was found to be equal to 11.

Different pH ranges have been reported in the previous works. The highest reduction of chromium was found at around 79% at pH 7 by using DC current 1.25 mA/cm^2 [39]. In addition, in another study for the removal of COD from the wastewater using electro-coagulation, the best pH was found around 7 with a COD removal of 75% [40]. Also, in a conducted experiment for the removal of colour, turbidity, and COD from wastewater by electrocoagulation, the best removal efficiency was found at around pH 8 [41]. For investigating the influence of pH on the removal efficiency in electrocoagulation, it has been proven that the best pH for reaching the best removal efficiency of reactive dye extraction from water (96%) is pH 6 [42]. All these studies show that the best pH range during the EC

experiment is a neutral range of pH (6–8). In this current study, also, 97% efficiency was reached in pH 7 after 20 min of contact; however, pH 11 showed the best result for this study. The best removal efficiency at pH is likely due to the increased formation of hydroxide ions, which enhance the precipitation of metal hydroxides and other contaminants, improving coagulation and flocculation processes.

Effect of Distance Between Electrodes

With the initial concentration of 50 mg/L and the pH of 11, a set of electrocoagulation tests were conducted to measure the effect of electrode distances. The same as the previous part, after 5, 10, 15, and 20 min and with 5, 10, and 15 mm distance between electrodes, samples measured with a spectrophotometer were filtered with the paper filter number 5, and the efficiency of work is shown in Figure 8.
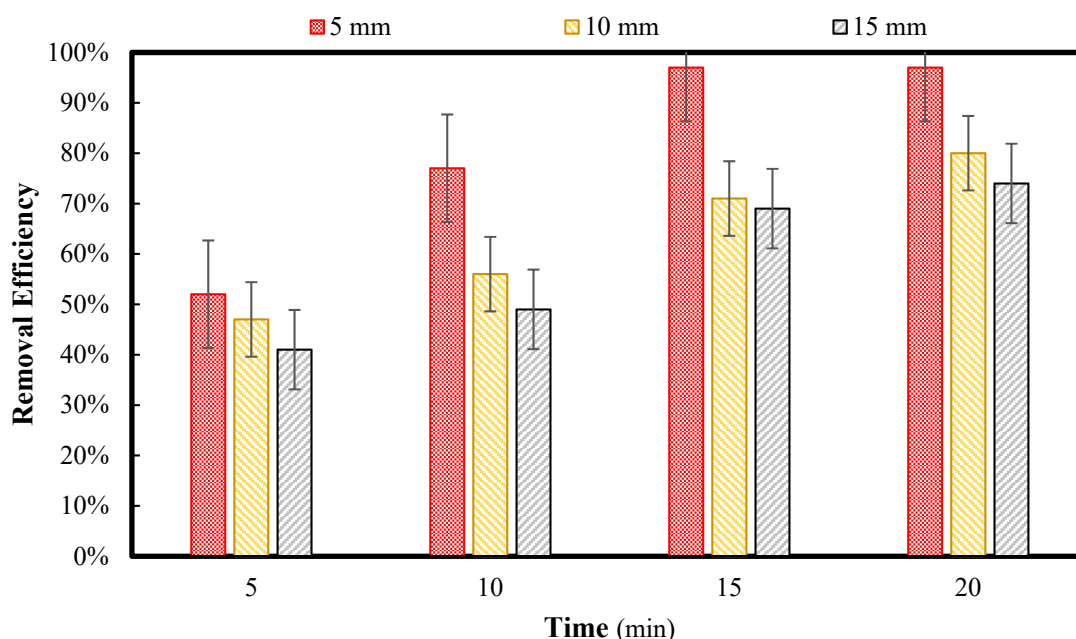

Figure 8. Effect of distance between electrodes on the EC test with 5, 10, and 15 mm of electrode distances in pH 11, after 5, 10, 15, and 20 min of the test.

The best performance was found in 5 mm distances between electrodes where 97% removal efficiency was reached after 15 min of contact time. This result showed a decrease in the efficiency when the electrode distances were adjusted to 10 and 15 mm. The best performance with 10 and 15 mm of electrode distances was found to be 80 and 74% after 20 min of contact time, respectively.

This parameter is investigated in many EC studies to examine its effect on removal efficiency. In a study of the removal of fluoride from groundwater, the effect of electrode distances was investigated. This study was conducted in a pH range from 3 to 9, with current density between 3 and 12 mA and 5 to 15 mm electrode distances, and the authors report that no changes occurred in the result by the changes in the distance between electrodes [43]. However, changes in the removal efficiency were reported with the changes in the distance between electrodes. In one study for the removal of heavy metals from water using the EC treatment method, inter-electrode distances started from 1 to 4 cm, and the best efficiency was investigated in 1 cm for the removal of Cr (96%), Ni (96.4%), Zn (99.9%), Cu (98%), and Pb (99.5%) [44]. The optimal removal efficiency in this condition is due to the stronger electric field, which boosts coagulant generation and speeds up the aggregation of contaminants.

Effect of Current Density

The next parameter investigated is the effect of current density on the removal efficiency of Montelukast Sodium (MS) from contaminated water. The C_0 for this test was 50 mg/L, the pH was 11, and the distance between electrodes was adjusted to 5 mm. Similarly to the previous section, samples were filtered using paper filter number 5 and then measured using the spectrophotometer after 5, 10, 15, and 20 min of contact time and with 10, 20, and 30 mA current density, and the results are displayed in Figure 9.
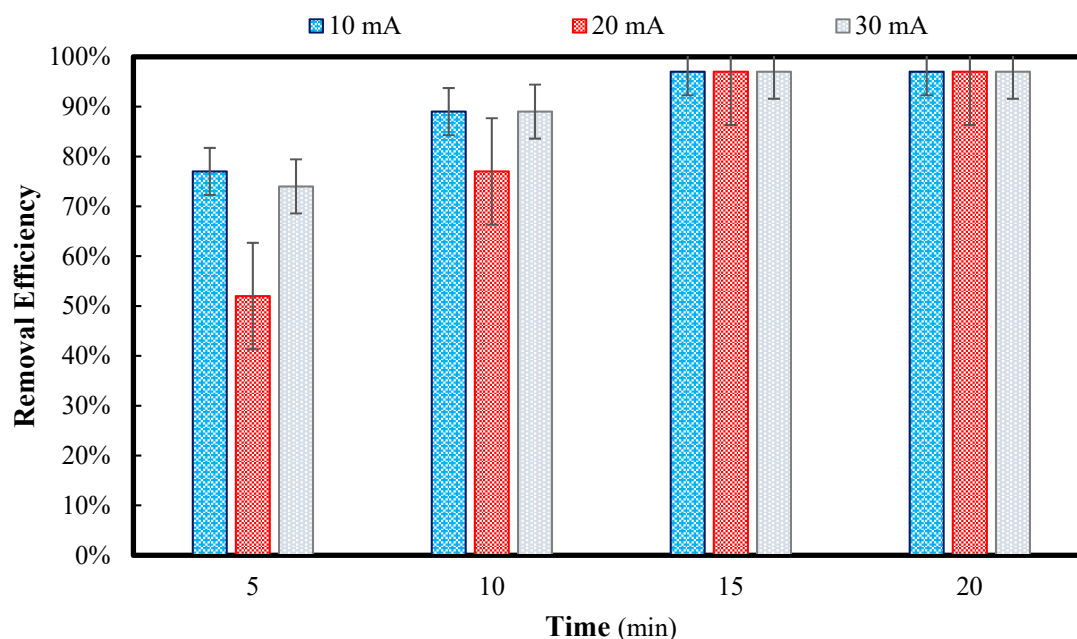

Figure 9. Effect of current density on EC test in 10, 20, and 30 mA current, in pH 11 and 5 mm distance between electrodes after 5, 10, 15, and 20 min run.

The results showed that with all tested current densities, which were 0.1, 0.2, and 0.3 A, the best removal efficiency was reached after 15 min of contact, which was 97%, and remained the same after 20 min of contact time. The best current density was 10 mA, then 30 mA with a very small difference, and then 20 mA had the lowest performance; however, despite the lowest performance of the current density of 20 mA, the experiments continued with the same current density as previous tests because even this current density reached 97% removal after 15 min of contact time.

A study investigating the effect of electric current on peat water treatment with EC was conducted in 2022. The result showed that after testing the current in 10, 14, and 18 mA, the most effective current density was found to be the last one [45]. In another study for the treatment of rice mill effluent, the best current density was found to be around 21 mA, and it was investigated that by increasing the current density, the removal efficiency would be decreased [46].

Effect of Time

The final parameter tested in the electrocoagulation section was the effect of time. With the initial concentration of 50 mg/L, and after the best conditions were found, which included a pH of 11, current density of 20 mA, and distance between electrodes of 5 mm, the experiments for the effect of time after 10, 20, 30, 40, 50, and 60 min were conducted. The detailed results of the experiments (after three repetitions to validate the result) are shown in Figure 10.
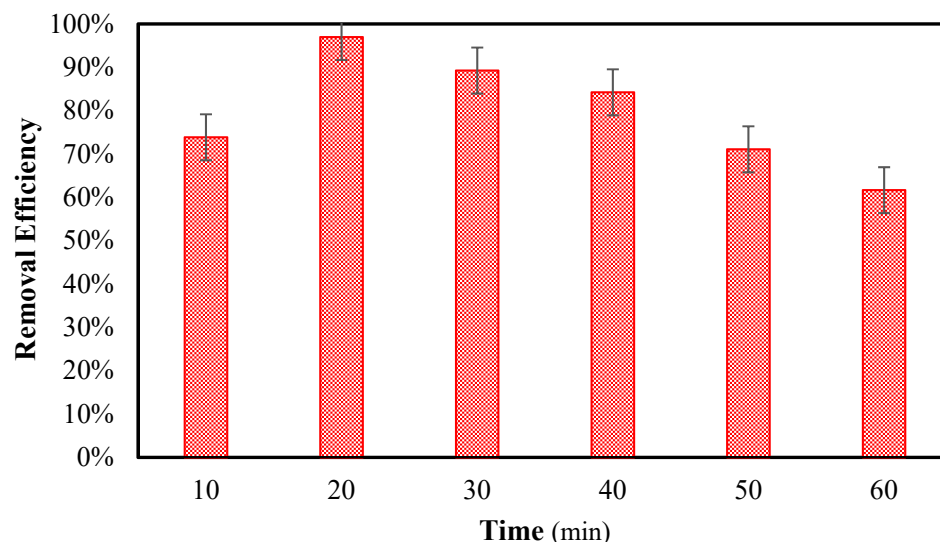
Figure 10. Effect of time on the best condition of EC test in pH 11, 5 mm of electrode distances, and 20 mA of current density after 10, 20, 30, 40, 50, and 60 min run.

Based on the results, it could be understood that the best efficiency was reached after 20 min of contact time, the same as in previous experiments. However, after 20 min, the efficiency of work started to decrease steadily, and 89, 84, and 71% removal efficiency were observed after 30, 40, and 50 min of contact between electrodes and water, respectively. The lowest removal efficiency in this part was reached after 1 h of contact time, and the percentage of 62% removal of MS from water. The reason behind the decrease after reaching 100% could be because of the presence of aluminium released to the water from aluminium electrodes, and it can be argued that the more contact between the electrode and water, the more aluminium ions are released into the water, and as a result, the removal efficiency was decreased. Using the aluminium electrodes as well, a study for the removal of Cu, Ni, and Zn was investigated after 75 min of EC process time; the best removal efficiency was found after 20 min, and then it started to decrease steadily [47].

3.2.2. Second Batch Tests

The last part of the current experiment is the adsorption batch test, which is the best condition found in the first phase of the experiment. The conditions are a pH of 3 and after 120 min of shaking time between the adsorbent (CFO-SS) and contaminated water. Different adsorbent dosages (0.05, 0.1, 0.2, 0.3, 0.4, and 0.5 g) were employed to measure the effect of the adsorbent dosage after 2 h of batch testing. The residual water after 60 min of the electrocoagulation test was measured with the pH metre, and the pH was found to be around 12. Due to the best performance of the adsorbent in the acidic phase, it was necessary to change the pH from 12 to 3 for the best removal efficiency. In this stage, acidification occurred using HCl to drop the pH to 3, and then the batch tests were started. The results are provided in Figure 11.

The best performance of the adsorbent was investigated with 0.5 g dosage of CFO-SS after 120 min at a pH of 3, and the removal efficiency was found to be 74%, which shows a good performance of the aluminium removal process from the EC residual water. The lowest removal was found with 0.05 g of activated sand, which shows that the lowest dosage of adsorbent showed a lower rate (34%) in the removal of MS.

To have a good comparison of the efficiency of this study with other methods of treatment for the removal of pharmaceuticals from the aqueous solution, Table 1 is provided. The other current methods for pharmaceutical removals like membranes, electrochemical methods, adsorption, and ion exchange are compared with this study, which shows the high performance of the adsorbent and electrocoagulation process with high removal efficiency.
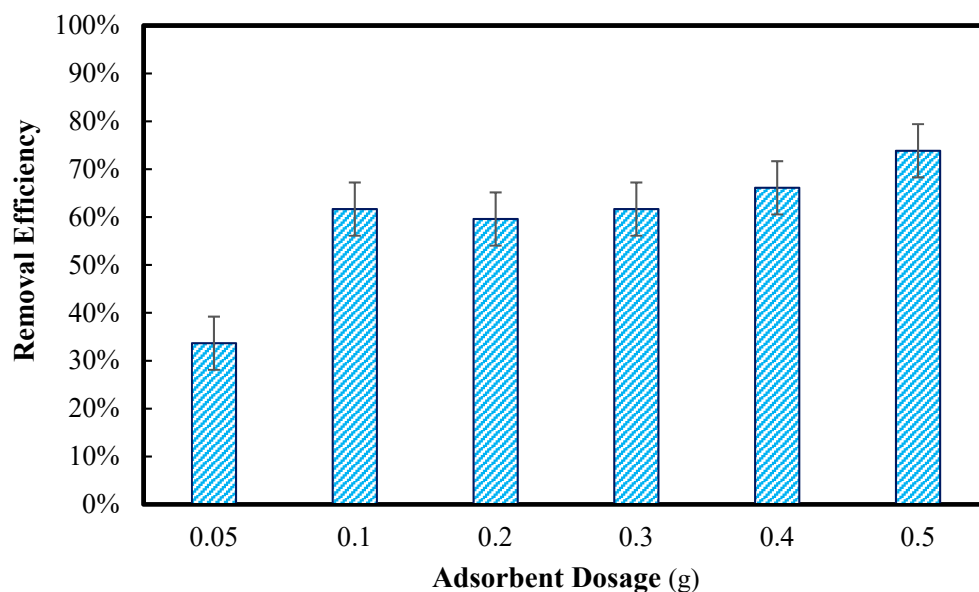
Figure 11. The removal efficiency of adsorption with EC residual water and the effect of adsorbent dosage on the removal in the best conditions (pH of 3, contact time of 120 min).

Table 1. Current methods of pharmaceutical pollutant removal from water.

Method	Pharmaceutical	Optimum Conditions	RE (%)	Ref.
Ultrafiltration Membrane	Sulfadiazine	pH: 7.5 time: 120 min feed conc.: 0.4 μmol/L	91.4	[48]
	Tetracycline	pH: 8.0 temp.: 25 °C feed conc.: 100 μg/L flux: 50 L.h^{-1} m^{-2}	>90	[49]
Nanofiltration Membrane	Amoxicillin	pH: 9.0 temp.: 298 K operating pressure: 2 MPa feed conc.: 20 ppm	56.4–99	[50]
Reverse Osmosis	Sulfamethoxazole	pH: 7.0 ± 0.1 temp.: 20 °C feed conc.: 100 μg/L	70–82	[51]
Electrocoagulation	Oxytetracycline Hydrochloride	Iron/aluminium anode (70 × 50 mm) Stainless steel cathode (70 × 50 mm) electrode distances: 5 cm current density: 20 mAcm^2 time: 120 min	82.9–93.1	[19]
	Ciprofloxacin (CIP)	Aluminium anode and cathode pH: 7.78 electrode distance: 1 cm time: 20 min current density: 12.5 mAcm^2	88.5	[52]
	Montelukast Sodium	Aluminium anode and cathode (110 × 55 mm) pH: 11 time: 20 min electrode distance: 5 mm current density: 20 mAcm^2	97	This study

Table 1. *Cont.*

Method	Pharmaceutical	Optimum Conditions	RE (%)	Ref.
Adsorption	Ibuprofen Naproxen Diclofenac	pH: 4–5 time: 60 min temperature: 24.85 °C	74.4 91.4 86.9	[53]
	Diclofenac	pH: 6 time: 120 min temperature: 25 °C	81	
	Montelukast Sodium	pH: 3 time: 120 min temperature: 25 °C adsorbent dosage: 0.1 g	99.5	This study

3.3. Sorption Isotherm and Kinetics

3.3.1. Isotherm Calculations

The distribution of pollutants on the solid phase at equilibrium, the maximum adsorption capacity, and the affinity of the adsorbent are all calculated using the adsorption isotherm. These isotherms are essential to characterise the interaction between the pollutants and the coated sand in the packed bed. Using the "solver" option nonlinear regression in Microsoft Excel Software 365, nonlinear versions of the Freundlich and Langmuir models are used to match the obtained sorption findings of MS adsorption by the synthesised coated sand. Table 2 displays R^2, the sum of squared errors (SSE), and the model constants.

Table 2. Isotherms models for the adsorption of MS.

Model	Parameter	Value
Freundlich	$Kf_{(mg/g)\,(L/mg)1/n}$ N R^2 SSE	3.886 2.179 0.736 99.840
Langmuir	$q_{m\,(mg/g)}$ $b_{(L/mg)}$ R^2 SSE	43.128 0.026 0.970 76.499

The findings indicate that the Freundlich interpretation is not as suitable for representing the measured data as the Langmuir model. Compared to the Freundlich model, the Langmuir model seems better suitable for measurement formulation, as indicated by the values of R2 and SSE (0.970 and 76.499, respectively). On the other hand, Figure 12 describes how the measurements and the Langmuir model matched; the maximum values of the capacity and affinity constant for the interaction of MS with the current sorbent were 43.128 mg/g and 0.026 L/mg, respectively; these values are near the maximum experiments (qe) of 48.49 mg/g.

For a better understanding of the reliability of the result of the isotherm model in this study, a comparison with the existing literature might be helpful. In this current study, the Langmuir model is predominant with $R^2 = 0.97$, and, compared to the previous study which was conducted by the authors with $R^2 = 0.995$ in the Langmuir model, there is a small difference [25]. Compared to other studies in the literature as well, a study for the removal of acetaminophen (ACE), cephalexin (CPX), and valsartan (VAL) from water, in the Langmuir model, R^2, was found 0.92, 0.91, and 0.84, respectively [2]. In another study for the removal of diclofenac (DCF) and trimethoprim (TMP) from water, the Langmuir isotherm shows that R^2 equals 0.99, and 0.98, respectively, using biochar as the adsorbent [54].
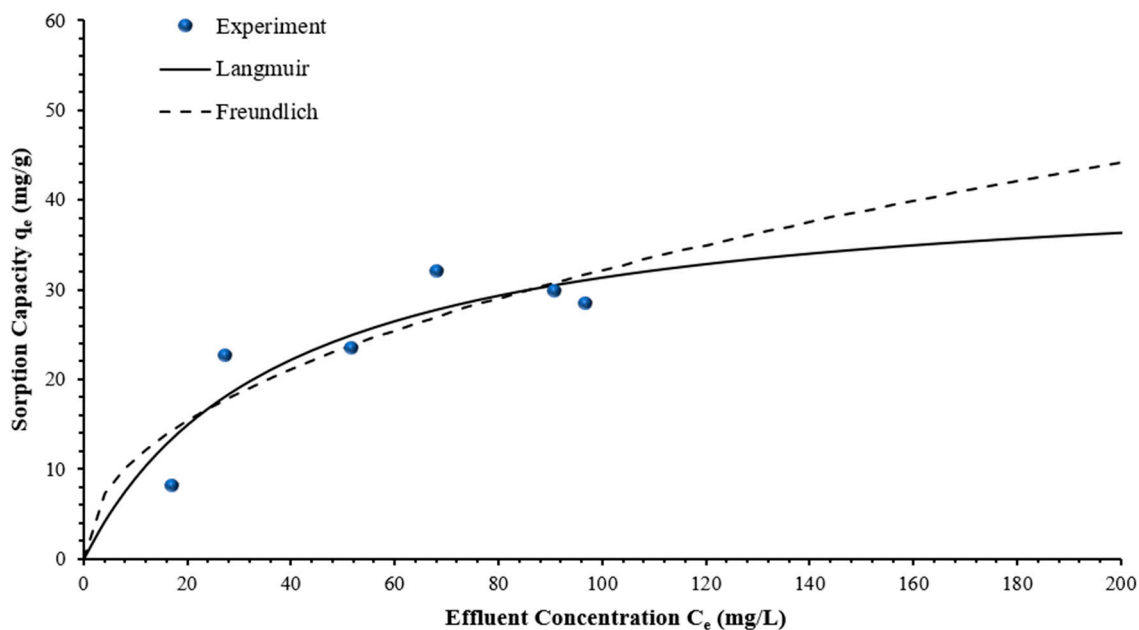
Figure 12. The isotherm models' rate constant using statistical data of MS sorption with activated sand.

3.3.2. Kinetic Calculations

Employing Microsoft Excel 365′s "Solver" tool, nonlinear analysis was used to fit kinetic studies of the fluctuation of MS adsorption with contact time onto the novel adsorbent at different initial concentrations of MS. Under the same ideal circumstances as the preceding batch tests, the kinetic experiments were conducted.

Table 3 displays the kinetic models' constants as determined by Equations (5) and (6), which are obtained from the fitting procedure. In addition, statistical measures such as the coefficient of determination (R^2) and the sum of squared error (SSE) are developed to characterise the convergence of the theoretical models with the experimental data.

Table 3. Kinetic parameters for CFO-SS-adsorbed Montelukast Sodium.

Model	Parameter	C_0 (mg/L)				
		50	**75**	**100**	**125**	**150**
Pseudo First Order	k_1 (min^{-1})	1.805	0.022	0.171	0.122	0.121
	q_e (mg/g)	16.803	23.839	32.140	28.116	28.178
	R^2	0.611	0.611	0.942	0.978	0.976
	SSE	153.795	153.795	52.025	14.479	15.791
Pseudo Second Order	$q_{exp.}$ (mg/g)	22.680	23.450	32.040	28.450	29.820
	k_2 (g/mg min)	0.002	0.001	0.009	0.007	0.007
	q_e (mg/g)	25.222	30.469	34.271	30.093	30.150
	R^2	0.985	0.988	0.965	0.995	0.996
	SSE	5.847	6.064	31.396	3.450	2.622

.Because it had the greatest R^2 and the shortest SSE, the Pseudo-Second-Order model, as shown by kinetic fitting in Table 3, was the most effective in describing the adsorption process of MS. The fact that the measured adsorbed quantity of MS (q_e) was nearly in line with the expected values further supports the applicability of the model. These findings verified that chemical bonds (i.e., chemisorption) are responsible for the MS clearance.

In the authors' previous published work using activated sand as the adsorbent, the kinetics were calculated, and Pseudo Second Order was predominant in that study. The R^2 was found to be 0.999, 0.981, 0.968, 0.981, and 0.991 for the initial Tetracycline (TC) concentration of 10, 50, 100, 150, and 200 mg/L [26].

3.4. Characterisation of the Adsorbent

3.4.1. X-Ray Diffraction (XRD)

The chemical composition of the used WPSA (wastepaper sludge ash) was examined using X-ray fluorescence analysis and XRF analysis. The results revealed that the primary oxide constituting the WPSA is CaO, which accounts for approximately 34% of the entire composition, as shown in Table 4 below. The sample characterised in the author's previous study is cited.

Table 4. XRF analysis for wastepaper sludge ash [26].

Chemical Consentient	Empirical Formula	Chemical Composition (*w/w*%)
Calcium oxide (lime)	CaO	34.01
Chlorine	Cl	8.78
Sulphate	SO_3	3.15
Silicon Dioxide (silica)	SiO_2	3.11
Aluminium Trioxide	Al_2O_3	3.08
Sodium Oxide	Na_2O	2.87
Phosphorus Pentoxide	P_2O_5	1.57
Titanium Dioxide	TiO_2	0.81
Potassium Oxide	K_2O	0.61
Magnesium Oxide	MgO	0.51
Iron (III) Oxide	Fe_2O_3	0.47

As shown in Figure 13, the XRD spectrum test for the (CFO-SS) was conducted. The PANalytical/X'Pert HighScore Plus programme was used to analyse the results of XRD powder diffraction measurements. The results showed the appearance of calcium ferric oxides on the sand following the modification process. After comparing the measurements to the Joint Committee on Powder Diffraction Standards (JCPDSs), it was discovered that the main component causing the peaks to appear was silica oxide.
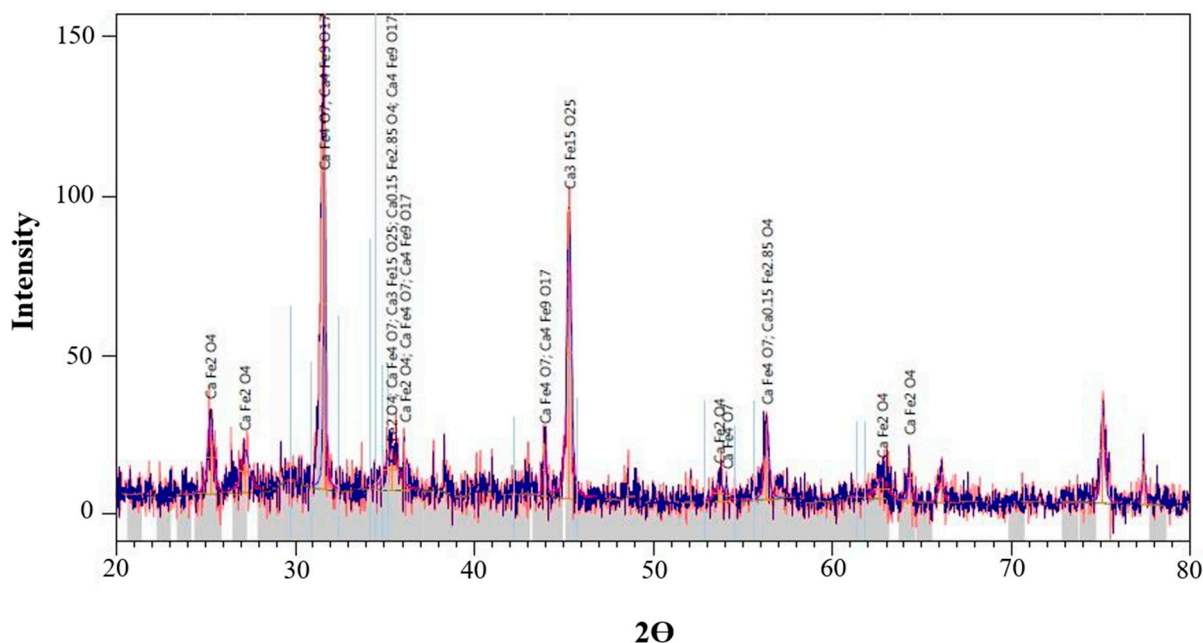

Figure 13. The XRD analysis for the activated sand.

The synthesis of ($Ca_4Fe_9O_{17}$, $CaFe_2O_4$, $CaFe_4O_7$, $Ca_{0.15}Fe_{2.85}O_4$, and $Ca_3Fe_{15}O_{25}$) was discovered by the X'Pert HighScore Plus software. These substances oversee the MS's

adsorption because they transform the unprocessed sand into a reactive medium that could capture the contaminants in an aqueous setting.

3.4.2. Scanning Electron Microscopy (SEM)

The morphology of raw sand, activated sand before interaction, activated sand after interaction with MS, and activated sand after interaction with the residual water after EC were investigated using the INCAx-act machine and using the xT microscope control tool, and the pictures are shown in Figure 14. The results showed that the sand's surface was smooth; however, the coated sand's enhanced surface roughness was caused by the calcium ferric oxides' immobilisation on the sand's surface, which attracted the pollutant in the first and second stage of the experiments to the coated sand.
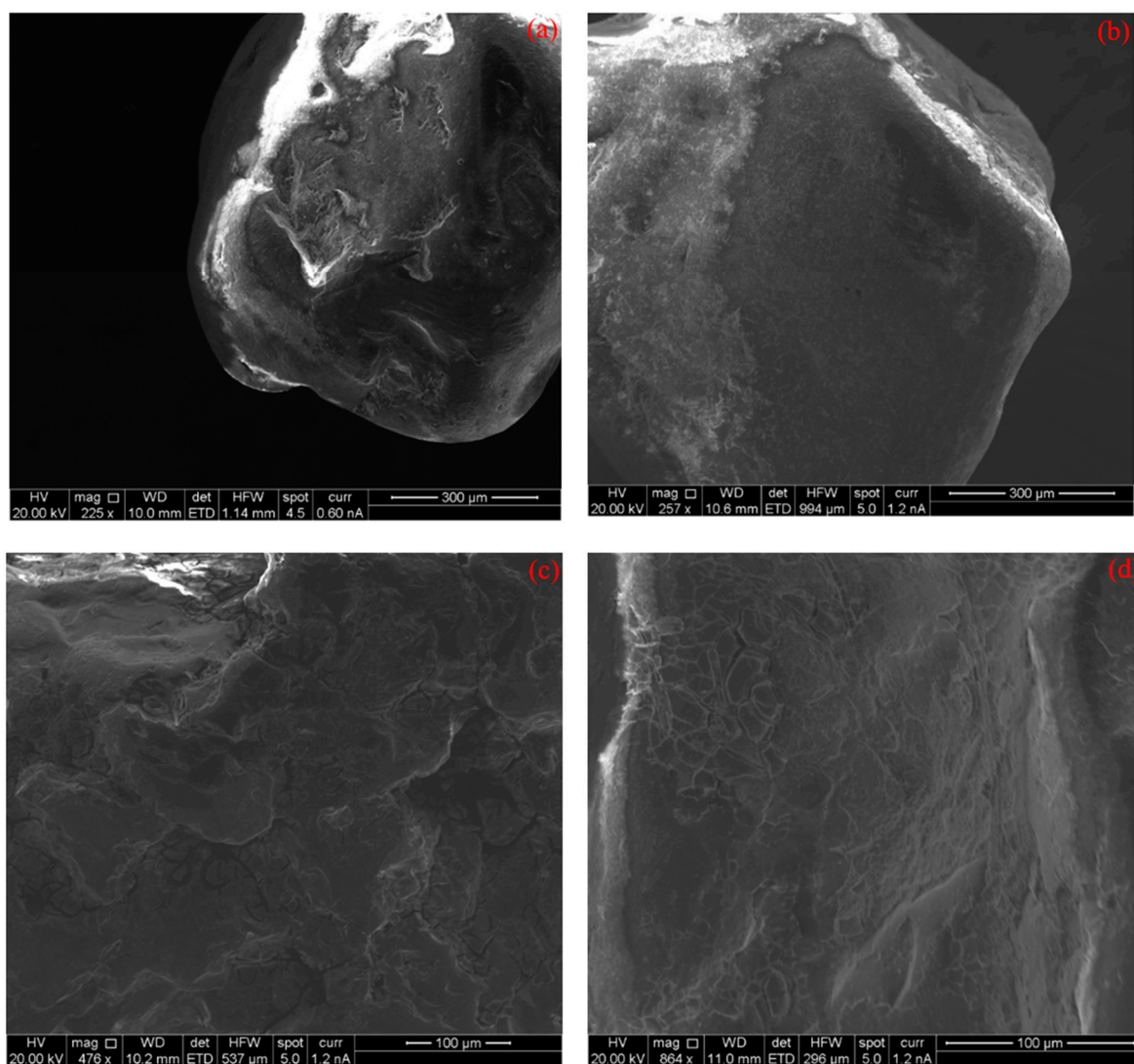

Figure 14. SEM pictures of raw sand (**a**), activated sand before interaction (**b**), activated sand after interaction with MS (**c**), and activated sand after interaction with the residual water after EC (**d**).

3.4.3. Energy-Dispersive X-Ray (EDX)

Energy-Dispersive X-ray Spectroscopy (EDX or EDS) is a powerful analytical technique used to identify the elemental composition of materials by measuring the energy and intensity of X-rays emitted from a sample. It is commonly coupled with Scanning Electron Microscopy (SEM) to provide detailed, localised chemical information at the micro to nanoscale, and the same machine (INCAx-act) has been used for this purpose via INCA

software. The results of raw sand and activated sand with calcium ferric oxide and a comparison between raw and activated sand in terms of chemical changes are shown in Figure 15. Moreover, the spectrum for activated sand after adsorption in the first and second stages of the experiment is illustrated in Figure 16.
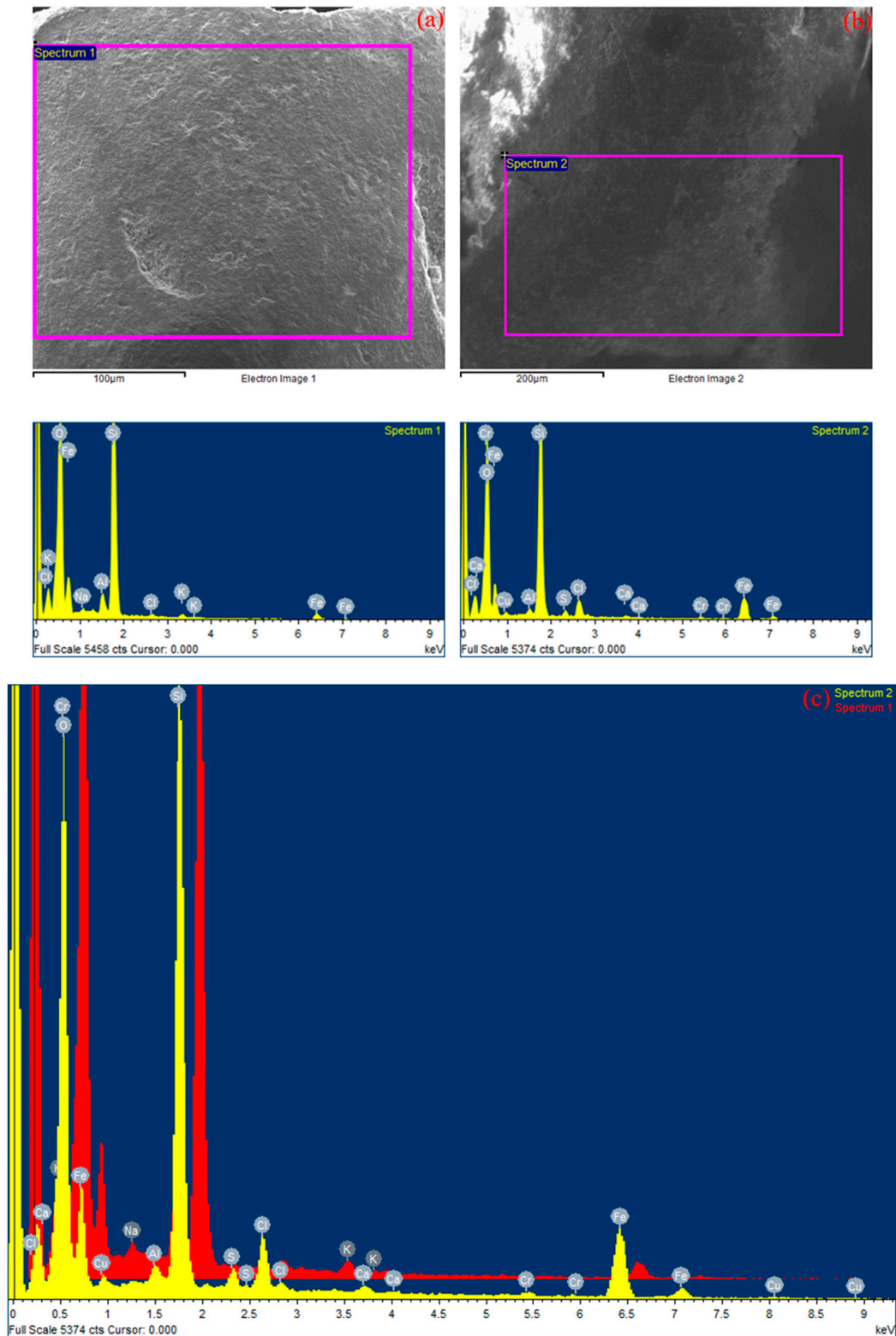

Figure 15. EDX analysis for the raw sand (**a**), the sand after activation (**b**), and the comparison of chemicals present in the raw and activated sand (**c**).
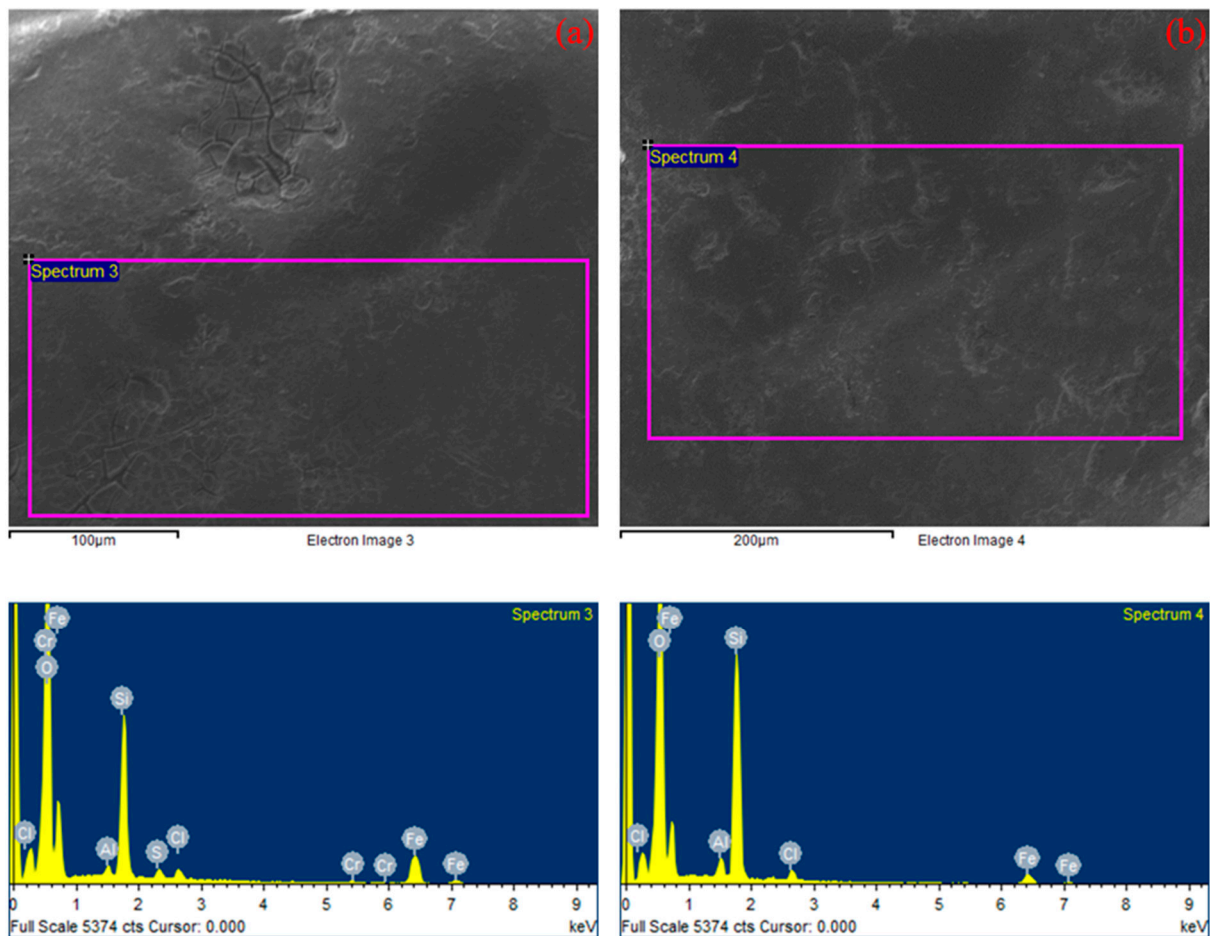
Figure 16. EDX analysis for the two samples after interaction with the pollutants: (**a**) activated sand after first adsorption batch test and (**b**) activated sand after the second adsorption batch test.

The raw sand is silica sand with the presence of silica (Si) and oxygen (O) and activated with calcium ferric oxide ($CaFe_2O_4$) to enhance the ability to adsorb the pollutant in the water, so the presence of Ca and Fe, and O, is expected. According to Figure 15, these chemicals are observed in the activated sand, which means the sand was activated properly. In Section c in Figure 15, two diagrams are also drawn together, and it can be understood from the figure that changes in chemical composition occurred during the activation stage.

After the adsorption process, chemical composition is also tested and observed in Figure 16. Spectrum 3 (Figure 16a) is for the adsorption bath test for MS removal, and Spectrum 4 (Figure 16b) is for after adsorption with EC residual water. It can be assumed from the pictures that electrocoagulation performed perfectly for pollutant removals, as there was no presence of S and Cr after EC, and the amount of Fe and Cr also declined after contact with electrodes. Therefore, the result shows that combining electrocoagulation and adsorption as a hybrid EC-A method was successful in terms of the removal of several chemical compositions.

3.4.4. Fourier Transform Infrared Spectroscopy (FT-IR)

Fourier Transform Infrared Spectroscopy (FTIR) is a key analytical tool used to identify and characterise chemical compounds by measuring the absorbance of infrared light across different wavenumbers, and in this study, an Agilent Technologies Cary 630 FTIR infrared spectrometer was utilised for this purpose.

Figure 17 shows the result of FTIR analysis for the raw and activated sand and the sand after each experiment stage. The highest pick is observed in all pictures in wavenumber around 1100 cm^{-1}. The C–O tensile vibrations and C–O rings coming from the deformation of C–C–H and C–O–H are responsible for the peaks at 1100 cm^{-1}. The absorbance also was around 0.04 in the raw sand, then it decreased to near zero after the activation, and, finally, it was around 0.02 after the absorption in the first and second stages of the experiment.
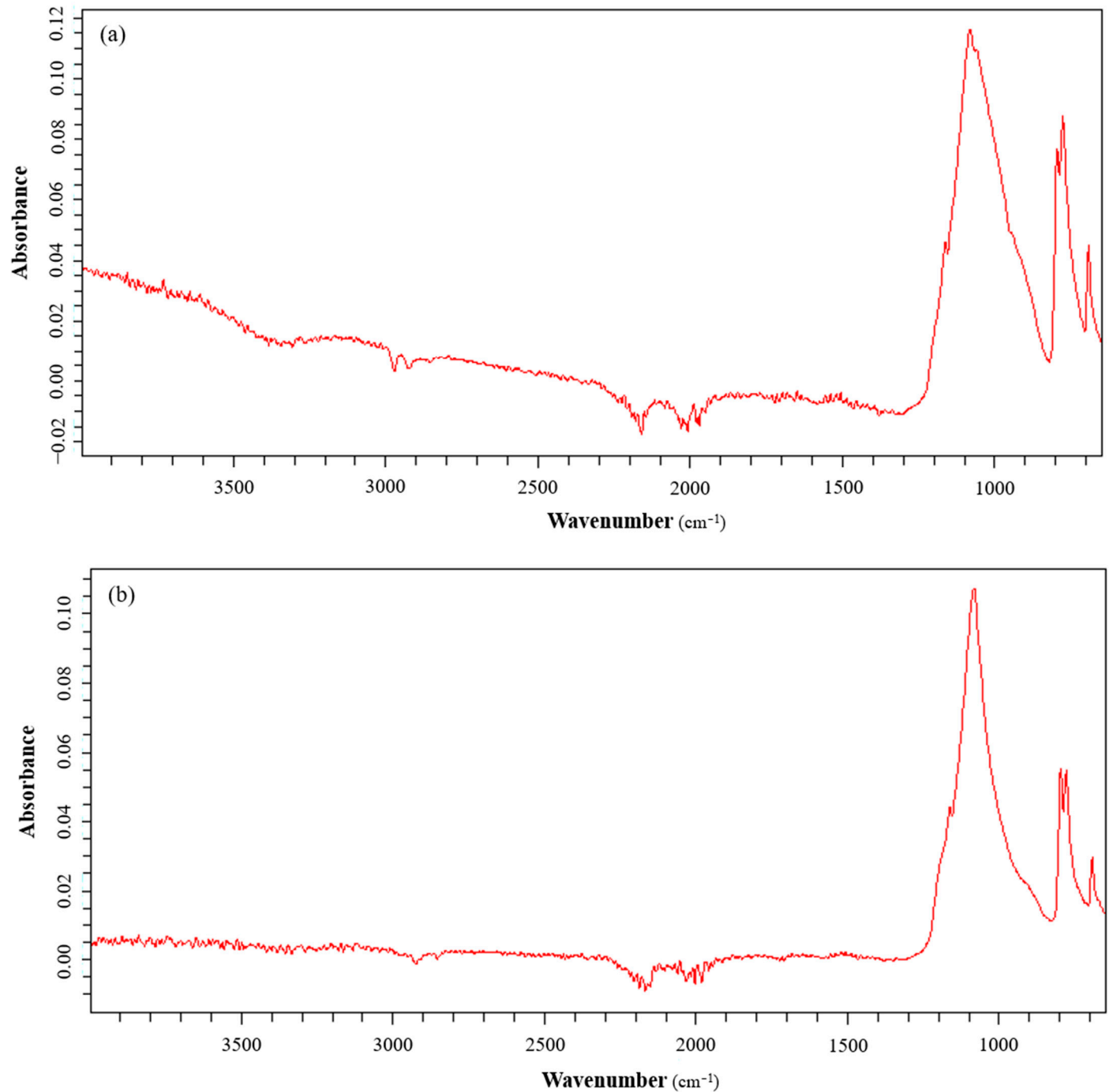

Figure 17. *Cont.*
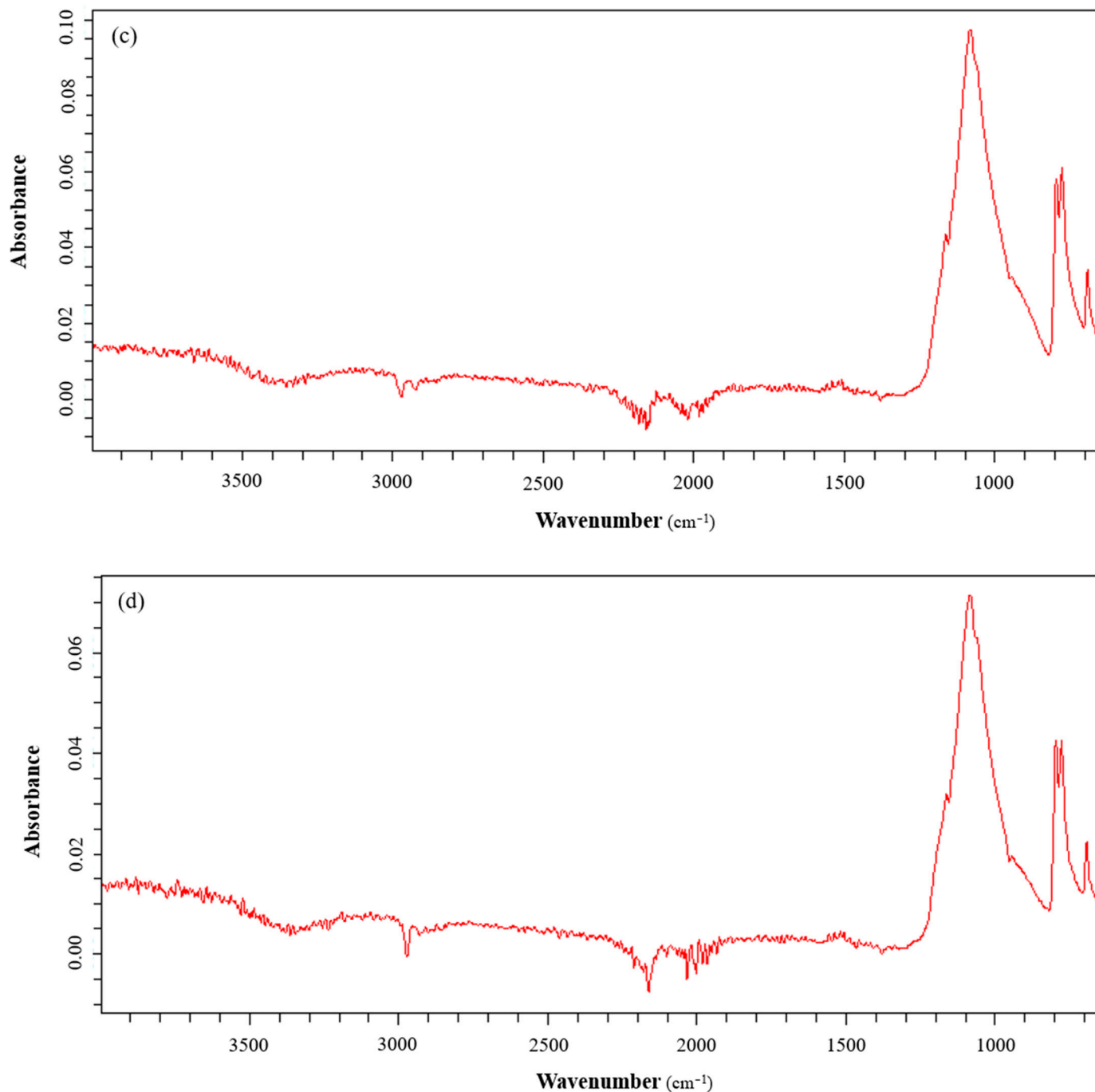
Figure 17. FT-IR analysis for the raw sand (**a**), activated sand with ferric oxide (**b**), the sand after interaction with MS (**c**), and the sand after interaction with the residual water of EC treatment (**d**).

3.5. Activated Sand Bench Cost Breakdown

The creation of this new adsorbent has a high cost because the process of creating coated sand requires the use of both materials and energy. The entire cost of the materials utilised could be used to determine the cost of materials. The recommended material costs are calculated from suppliers and commercial rates. On the other hand, the specific heat capacity approach has been used to calculate the energy needed for the coated sand production process. The process of producing coated sand involves the use of a mixer and dryer, which results in the need for energy-intensive mixing and drying procedures. Based on the power parameters of the mixer supplied by the vendor during the mixing time, a field mixer that uses 1.8 kW per 250 kg of sand might be used in the manufacturing of

1000 kg of coated sand. The following computations have been used to estimate the oven's energy consumption:

To calculate the energy required to heat 1000 kg of sand from 18 °C (measured sand temperature) to 95 °C for 12 h, it is required to use the specific heat capacity of sand and the following formula (Equation (7)):

$$\text{Energy (Q)} = \text{mass (m)} \times \text{specific heat capacity (c)} \times \text{change in temperature (}\Delta T) \quad (7)$$

Assume that the oven maintains a constant temperature of 95 °C during the 12 h heating period. Therefore, the change in temperature (ΔT) is as follows:

$$\Delta T = 95\,°C - 18\,°C = 77\,°C$$

To calculate the mass of sand, the density of sand is 1600 kg/m^3. Therefore, the volume of 1000 kg of sand is as follows:

$$\text{Volume} = \text{Mass/Density} = 1000\,\text{kg}/1600\,\text{kg/m}^3 = 0.625\,\text{m}^3$$

Oven capacity (Genlab SDO/18H/GDIG) is 425 L; if the sand fills 80% of the entire oven capacity, then each batch can dry 0.34 m^3. Accordingly, two batches are required to treat the 1000 kg of sand, 500 kg each.

The specific heat capacity of sand varies depending on its composition, but a reasonable average value is around 0.8 J/g°C. Therefore, the energy required to heat 1 kg of sand by 1 degree Celsius is as follows:

c = 0.83 J/g°C = 830 J/kg°C [55]

The total energy required to heat 1000 kg of sand by 77 degrees Celsius is as follows:

$$Q = m \times c \times \Delta T = 500\,\text{kg} \times 830\,\text{J/kg}°C \times 77\,°C = 31{,}955{,}000\,\text{J}$$

Next, it is required to calculate the energy required to maintain the sand at 95 °C for 12 h; note that oven power at 95 °C is 1.5 kW.

E = P × t where E is the energy, P is power in Watts (W), and t is time in h (hours);
E = 1.5 kW × 12 h × 1000 (to convert to watts);
E = 18,000,000 J.
To calculate the total energy required to keep 500 kg of sand dry at 95 °C, the following is calculated:

$$\text{Total energy} = 31{,}955{,}000\,\text{J} + 18{,}000{,}000\,\text{J}$$

$$\text{Total energy} = 49{,}955{,}000\,\text{J (49,955 kJ)}$$

$$\text{Total energy} = 13.88\,\text{kWh}$$

To calculate the cost of this electricity at a unit rate of 34 pence per kWh (according to the energy prices/uk.gov),

$$\text{Cost} = 13.88\,\text{kWh} \times 34\,\text{pence/kWh}$$

$$\text{Cost} = £4.72$$

For two batches, the cost is GBP 9.44.

Therefore, the cost of electricity required to heat 1000 kg of sand from 18 °C to 95 °C and keep it at 95 °C for 12 h, using 80% of a 425 L oven with a power of 1.5 kW at 95 °C, is GBP 9.44.

The power required for mixing the sand: 1.8 kW × 3 h × 4 batches = 21.6 kWh;
Mixing cost for 1000 kg of sand = 21.6 kWh × 34 pence/kWh = GBP 7.34;
Total mixing and drying cost: GBP 16.78/1000 kg of coated sand;
For 1 kg: the cost is GBP 1.678.

The bench costs of the used materials and energy used to produce 1 kg of the reactive sand are shown below in Table 5:

Table 5. Activated sand cost breakdown.

Seq.	Item	Unit	Quantity	Unit Cost (GBP)	Total Cost (GBP)
1.	Quartz Sand	kg	1	GBP 0.11	GBP 0.11
2.	FeCl$_3$	Kg	1	GBP 3.63	GBP 3.63
3.	Ethylene Glycol	g	1825	0.0007	GBP 1.28
4.	Mixing and energy cost for 1 kg of coated sand	Each	Each	GBP 1.678	GBP 1.678
	Cost of materials + Energy				GBP 6.698

4. Conclusions

This work addressed a major environmental concern regarding pharmaceutical pollutants by successfully demonstrating the efficacy of a hybrid electrocoagulation–adsorption (EC-A) technique for the removal of Montelukast Sodium (MS) from contaminated water. The tests were conducted in three different stages: adsorption (first stage), electrocoagulation (second stage), and adsorption with the EC residual water (third stage). The crystalline structure of the adsorbent was analysed using X-ray Diffraction (XRD), the elemental composition was determined using Energy-Dispersive X-ray Spectroscopy (EDX), the surface morphology of the adsorbent materials was examined using Scanning Electron Microscopy (SEM), and the functional groups present in the adsorbent before and after interaction with the pollutants were identified using Fourier Transform Infrared Spectroscopy (FTIR). These methods offered a thorough understanding of the characteristics and efficiency of the adsorbent substances employed in the EC-A procedure.

The ideal parameters for the adsorption phase were determined to be a pH of 3 and a contact duration of 120 min. With the starting MS concentration of 50 mg/L, the greatest removal effectiveness of 99.5% was obtained under these conditions by utilising different dosages of CFO-SS adsorbent (0.05, 0.1, and 0.15 g). This suggests that acidic conditions greatly increase the adsorption capacity of MS. The electrocoagulation phase identified the best operational parameters at a pH of 11, a current density of 20 mA, and an electrode distance of 5 mm. This configuration resulted in a remarkable 97% removal efficiency after just 20 min of contact time, showcasing the rapid effectiveness of electrocoagulation in treating pharmaceutical contaminants. Finally, in the adsorption with the residual water from the electrocoagulation process, the residual water's pH was adjusted to 3 from around 12 using HCl, which further enhanced the removal efficiency to 74% with the 0.5 g adsorbent dosages.

It is advised that future research investigate the reusability and long-term stability of the adsorbent materials utilised in the EC-A method, as well as the effectiveness of other pharmaceutical pollutants removed under comparable circumstances. This could offer a more thorough comprehension of the process's suitability for different types of contaminants. The focus on a single pharmaceutical component, which might not accurately reflect the intricacies of real-world wastewater settings, was another research limitation. Further research, including a wider range of contaminants and actual wastewater samples, is therefore advised to verify the results and improve the value of the EC-A method in a variety of environmental settings. In addition, it is recommended to consider the presence of aluminium as a byproduct after electrocoagulation in the third stage of the experiment and conduct further research to determine the byproduct of the experiment.

Author Contributions: Conceptualization, S.M. and K.S.H.; Methodology, S.M. and K.S.H.; Software, S.M., O.A.-H. and A.M.; Validation, K.S.H. and O.A.-H.; Formal analysis, S.M. and K.S.H.; Investigation, S.M. and K.S.H.; Resources, K.S.H. and O.A.-H.; Data curation, S.M. and K.S.H.; Writing—original draft, S.M.; Writing—review and editing, S.M., K.S.H., O.A.-H. and A.M.; Supervision, K.S.H. All authors have read and agreed to the published version of the manuscript.

Funding: This research received no external funding.

Institutional Review Board Statement: Not applicable.

Informed Consent Statement: Not applicable.

Data Availability Statement: The data presented in this study are included in the article. Further inquiries can be directed to the corresponding author.

Conflicts of Interest: The authors declare no conflicts of interest.

References

1. Sheikh, S.; Naghizadeh-Dehno, O.; Mirkhalafi, S.; Ghashang, M. Magnetic heterogenization of supramolecular carbohydrates for the efficient adsorption of heavy metals removal from wastewater. *Inorg. Chem. Commun.* **2024**, *168*, 112835. [CrossRef]
2. Grisales-Cifuentes, C.M.; Serna Galvis, E.A.; Porras, J.; Flórez, E.; Torres-Palma, R.A.; Acelas, N. Kinetics, isotherms, effect of structure, and computational analysis during the removal of three representative pharmaceuticals from water by adsorption using a biochar obtained from oil palm fiber. *Bioresour. Technol.* **2021**, *326*, 124753. [CrossRef] [PubMed]
3. Küster, A.; Adler, N. Pharmaceuticals in the environment: Scientific evidence of risks and its regulation. *Philos. Trans. R. Soc. B Biol. Sci.* **2014**, *369*, 20130587. [CrossRef] [PubMed]
4. Hu, G.; Chen, S.; Mu, S. Characteristics of concentrations of antibiotics in typical drinking water sources in a city in Jiangsu Province. *Water Resour. Prot.* **2016**, *32*, 84–88.
5. Chen, M.; Ren, L.; Qi, K.; Li, Q.; Lai, M.; Li, Y.; Li, X.; Wang, Z. Enhanced removal of pharmaceuticals and personal care products from real municipal wastewater using an electrochemical membrane bioreactor. *Bioresour. Technol.* **2020**, *311*, 123579. [CrossRef]
6. Alenzi, A.; Hunter, C.; Spencer, J.; Roberts, J.; Craft, J.; Pahl, O.; Escudero, A. Pharmaceuticals effect and removal, at environmentally relevant concentrations, from sewage sludge during anaerobic digestion. *Bioresour. Technol.* **2021**, *319*, 124102. [CrossRef]
7. Xu, W.; Zou, R.; Jin, B.; Zhang, G.; Su, Y.; Zhang, Y. The ins and outs of pharmaceutical wastewater treatment by microbial electrochemical technologies. *Sustain. Horiz.* **2022**, *1*, 100003. [CrossRef]
8. Al-Qodah, Z.; Al-Zghoul, T.M.; Jamrah, A. The performance of pharmaceutical wastewater treatment system of electrocoagulation assisted adsorption using perforated electrodes to reduce passivation. *Environ. Sci. Pollut. Res.* **2024**, *31*, 20434–20448. [CrossRef]
9. Mariam, T.; Nghiem, L.D. Landfill leachate treatment using hybrid coagulation-nanofiltration processes. *Desalination* **2010**, *250*, 677–681. [CrossRef]
10. Qu, J.G.; Li, N.N.; Liu, B.J.; He, J.X. Preparation of BiVO4/bentonite catalysts and their photocatalytic properties under simulated solar irradiation. *Mater. Sci. Semicond. Process.* **2013**, *16*, 99–105. [CrossRef]
11. Mousazadeh, M.; Alizadeh, S.M.; Frontistis, Z.; Kabdaşlı, I.; Karamati Niaragh, E.; Al Qodah, Z.; Naghdali, Z.; Mahmoud, A.E.; Sandoval, M.A.; Butler, E.; et al. Electrocoagulation as a Promising Defluoridation Technology from Water: A Review of State of the Art of Removal Mechanisms and Performance Trends. *Water* **2021**, *13*, 656. [CrossRef]
12. Al-Qodah, Z.; Al-qudah, Y.; Omar, W. On the performance of electrocoagulation assisted biological treatment processes A review on the state of the art. *Environ. Sci. Pollut. Res.* **2019**, *26*, 28689–28713. [CrossRef] [PubMed]
13. Al-Qodah, Z.; Al-qudah, Y.; Assirey, E. Combined biological wastewater treatment with electrocoagulation as a post-polishing process: A review. *Sep. Sci. Technol.* **2019**, *55*, 2334–2352. [CrossRef]
14. Chandra, S.; Dohare, D.; Kotiya, A. Study of electrocoagulation process for removal of heavy metals from industrial wastewater A review. *Int. J. Eng. Res. Technol.* **2020**, *9*, 993–999.
15. Faraj, H.; Jamrah, A.; Al-Omari, S.; Al-Zghoul, T.M. Optimization of an electrocoagulation-assisted adsorption treatment system for dairy wastewater. *Case Stud. Chem. Environ. Eng.* **2024**, *9*, 100574. [CrossRef]
16. Bhagawati, P.B.; Lokeshappa, B.; Malekdar, F.; Sapate, S.; Adeogun, A.I.; Chapi, S.; Goswami, L.; Mirkhalafi, S.; Sillanpää, M. Prediction of electrocoagulation treatment of tannery wastewater using multiple linear regression based ANN: Comparative study on plane and punched electrodes. *Desalin. Water Treat.* **2024**, *319*, 100530. [CrossRef]
17. Bajpai, M.; Katoch, S.S.; Kadier, A.; Ma, P.-C. Treatment of pharmaceutical wastewater containing cefazolin by electrocoagulation (EC): Optimization of various parameters using response surface methodology (RSM), kinetics and isotherms study. *Chem. Eng. Res. Des.* **2021**, *176*, 254–266. [CrossRef]
18. Nariyan, E.; Aghababaei, A.; Sillanpää, M. Removal of pharmaceutical from water with an electrocoagulation process; effect of various parameters and studies of isotherm and kinetic. *Sep. Purif. Technol.* **2017**, *188*, 266–281. [CrossRef]

19. Ensano, B.M.B.; Borea, L.; Naddeo, V.; Belgiorno, V.; de Luna, M.D.G.; Balakrishnan, M.; Ballesteros, F.C., Jr. Applicability of the electrocoagulation process in treating real municipal wastewater containing pharmaceutical active compounds. *J. Hazard. Mater.* **2019**, *361*, 367–373. [CrossRef]

20. Kumari, S.; Kumar, R.N. River water treatment using electrocoagulation for removal of acetaminophen and natural organic matter. *Chemosphere* **2021**, *273*, 128571. [CrossRef]

21. Yegane Badi, M.; Azari, A.; Pasalari, H.; Esrafili, A.; Farzadkia, M. Modification of activated carbon with magnetic Fe_3O_4 nanoparticle composite for removal of ceftriaxone from aquatic solutions. *J. Mol. Liq.* **2018**, *261*, 146–154. [CrossRef]

22. Khaledi, K.; Valdes Labrada, G.M.; Soltan, J.; Predicala, B.; Nemati, M. Adsorptive removal of tetracycline and lincomycin from contaminated water using magnetized activated carbon. *J. Environ. Chem. Eng.* **2021**, *9*, 105998. [CrossRef]

23. Mondal, S.; Patel, S.; Majumder, S.K. Bio-extract assisted in-situ green synthesis of Ag-RGO nanocomposite film for enhanced naproxen removal. *Korean J. Chem. Eng.* **2020**, *37*, 274–289. [CrossRef]

24. Siciliano, A.; Guida, M.; Iesce, M.R.; Libralato, G.; Temussi, F.; Galdiero, E.; Carraturo, F.; Cermola, F.; DellaGreca, M. Ecotoxicity and photodegradation of Montelukast (a drug to treat asthma) in water. *Environ. Res.* **2021**, *202*, 111680. [CrossRef] [PubMed]

25. Al-Hashimi, O.; Hashim, K.; Loffill, E.; Nakouti, I.; Faisal, A.A.H.; Čebašek, T.M. Eco-friendly remediation of tetracycline antibiotic from polluted water using waste-derived surface re-engineered silica sand. *Sci. Rep.* **2023**, *13*, 13148. [CrossRef]

26. Al-Hashimi, O.; Hashim, K.; Loffill, E.; Nakouti, I.; Faisal, A.A.H.; Čebašek, T.M. Kinetic and Equilibrium Isotherm Studies for the Removal of Tetracycline from Aqueous Solution Using Engineered Sand Modified with Calcium Ferric Oxides. *Environments* **2023**, *10*, 7. [CrossRef]

27. Faisal, A.A.H.; Shihab, A.H.; Naushad, M.; Ahamad, T.; Sharma, G.; Al-Sheetan, K.M. Green synthesis for novel sorbent of sand coated with (Ca/Al)-layered double hydroxide for the removal of toxic dye from aqueous environment. *J. Environ. Chem. Eng.* **2021**, *9*, 105342. [CrossRef]

28. Liu, S.; Pan, M.; Feng, Z.; Qin, Y.; Wang, Y.; Tan, L.; Sun, T. Ultra-high adsorption of tetracycline antibiotics on garlic skin-derived porous biomass carbon with high surface area. *New J. Chem.* **2020**, *44*, 1097–1106. [CrossRef]

29. Unuabonah, E.; Onah, L.; Adeyemi, O. Multistage Optimization of the Adsorption of Methylene Blue Dye onto Defatted Carica papaya Seeds. *Chem. Eng. J.* **2009**, *155*, 567–579. [CrossRef]

30. Al Juboury, M.F.; Alshammari, M.H.; Al-Juhaishi, M.R.; Naji, L.A.; Faisal, A.A.H.; Naushad, M.; Lima, E.C. Synthesis of composite sorbent for the treatment of aqueous solutions contaminated with methylene blue dye. *Water Sci. Technol.* **2020**, *81*, 1494–1506. [CrossRef]

31. Simonin, J.-P. On the comparison of pseudo-first order and pseudo-second order rate laws in the modeling of adsorption kinetics. *Chem. Eng. J.* **2016**, *300*, 254–263. [CrossRef]

32. Ahmed, I.; Jhung, S.H. Applications of metal-organic frameworks in adsorption/separation processes via hydrogen bonding interactions. *Chem. Eng. J.* **2017**, *310*, 197–215. [CrossRef]

33. Carrasco, J.; Klimeš, J.; Michaelides, A. The role of van der Waals forces in water adsorption on metals. *J. Chem. Phys.* **2013**, *138*, 024708. [CrossRef] [PubMed]

34. Adamczyk, Z. Particle adsorption and deposition: Role of electrostatic interactions. *Adv. Colloid Interface Sci.* **2003**, *100–102*, 267–347. [CrossRef]

35. Padmavathy, K.S.; Madhu, G.; Haseena, P.V. A study on Effects of pH, Adsorbent Dosage, Time, Initial Concentration and Adsorption Isotherm Study for the Removal of Hexavalent Chromium (Cr (VI)) from Wastewater by Magnetite Nanoparticles. *Procedia Technol.* **2016**, *24*, 585–594. [CrossRef]

36. Ezeh, K.; Ogbu, I.; Akpomie, K.; Ojukwu, N.; Ibe, J. Utilizing the Sorption Capacity of Local Nigerian Sawdust for Attenuation of Heavy Metals from Solution: Isotherm, Kinetic, and Thermodynamic Investigations. *Pac. J. Sci. Technol.* **2017**, *18*, 251–264.

37. Okareh, O.T.; Timothy, A.; Dada, A.O. Adsorption of Chromium Ion from Industrial Effluent Using Activated Carbon Derived from Plantain. *Am. J. Environ. Prot.* **2015**, *4*, 7–20.

38. Lu, J.; Zhang, P.; Li, J. Electrocoagulation technology for water purification: An update review on reactor design and some newly concerned pollutants removal. *J. Environ. Manag.* **2021**, *296*, 113259. [CrossRef]

39. Prasetyaningrum, A.; Jos, B.; Dharmawan, Y.; Praptyana, I. The Effect of pH and Current Density on Electrocoagulation Process for Degradation of Chromium (VI) in Plating Industrial Wastewater. *J. Phys. Conf. Ser.* **2019**, *1295*, 012064. [CrossRef]

40. Syaichurrozi, I.; Sarto, S.; Sediawan, W.B.; Hidayat, M. Effect of Current and Initial pH on Electrocoagulation in Treating the Distillery Spent Wash with Very High Pollutant Content. *Water* **2021**, *13*, 11. [CrossRef]

41. Ebba, M.; Asaithambi, P.; Alemayehu, E. Investigation on operating parameters and cost using an electrocoagulation process for wastewater treatment. *Appl. Water Sci.* **2021**, *11*, 175. [CrossRef]

42. Hashim, K.; Hashim, A.; Zubaidi, S.; Kot, P.; Kraidi, L.; Alkhaddar, R.; Shaw, A.; Alwash, R. Effect of initial pH value on the removal of reactive black dye from water by electrocoagulation (EC) method. *J. Phys. Conf. Ser.* **2019**, *1294*, 072017. [CrossRef]

43. Kim, K.-J.; Baek, K.; Ji, S.; Cheong, Y.; Yim, G.; Jang, A. Study on electrocoagulation parameters (current density, pH, and electrode distance) for removal of fluoride from groundwater. *Environ. Earth Sci.* **2015**, *75*, 45. [CrossRef]

44. Bhagawan, D.; Poodari, S.; Pothuraju, T.; Srinivasulu, D.; Shankaraiah, G.; Yamuna Rani, M.; Himabindu, V.; Vidyavathi, S. Effect of operational parameters on heavy metal removal by electrocoagulation. *Environ. Sci. Pollut. Res.* **2014**, *21*, 14166–14173. [CrossRef]

45. Amri, I.; Herman, S.; Fadhlah Ramadan, A.; Hamzah, N. Effect of electrode and electric current on peat water treatment with continuous electrocoagulation process. *Mater. Today Proc.* **2022**, *63*, S520–S525. [CrossRef]

46. Anuf, A.R.; Ramaraj, K.; Sivasankarapillai, V.S.; Dhanusuraman, R.; Maran, J.P.; Rajeshkumar, G.; Rahdar, A.; Díez-Pascual, A.M. Optimization of electrocoagulation process for treatment of rice mill effluent using response surface methodology. *J. Water Process Eng.* **2022**, *49*, 103074. [CrossRef]

47. Mouedhen, G.; Feki, M.; Wery, M.D.P.; Ayedi, H.F. Behavior of aluminum electrodes in electrocoagulation process. *J. Hazard. Mater.* **2008**, *150*, 124–135. [CrossRef]

48. Zhou, A.; Jia, R.; Wang, Y.; Sun, S.; Xin, X.; Wang, M.; Zhao, Q.; Zhu, H. Abatement of sulfadiazine in water under a modified ultrafiltration membrane (PVDF-PVP-TiO2-dopamine) filtration-photocatalysis system. *Sep. Purif. Technol.* **2020**, *234*, 116099. [CrossRef]

49. Liao, Z.; Nguyen, M.N.; Wan, G.; Xie, J.; Ni, L.; Qi, J.; Li, J.; Schäfer, A.I. Low pressure operated ultrafiltration membrane with integration of hollow mesoporous carbon nanospheres for effective removal of micropollutants. *J. Hazard. Mater.* **2020**, *397*, 122779. [CrossRef]

50. Moarefian, A.; Golestani, H.A.; Bahmanpour, H. Removal of amoxicillin from wastewater by self-made Polyethersulfone membrane using nanofiltration. *J. Environ. Health Sci. Eng.* **2014**, *12*, 127. [CrossRef]

51. Kimura, K.; Toshima, S.; Amy, G.; Watanabe, Y. Rejection of neutral endocrine disrupting compounds (EDCs) and pharmaceutical active compounds (PhACs) by RO membranes. *J. Membr. Sci.* **2004**, *245*, 71–78. [CrossRef]

52. Ahmadzadeh, S.; Asadipour, A.; Pournamdari, M.; Behnam, B.; Rahimi, H.R.; Dolatabadi, M. Removal of ciprofloxacin from hospital wastewater using electrocoagulation technique by aluminum electrode: Optimization and modelling through response surface methodology. *Process Saf. Environ. Prot.* **2017**, *109*, 538–547. [CrossRef]

53. Husein, D.Z.; Hassanien, R.; Al-Hakkani, M.F. Green-synthesized copper nano-adsorbent for the removal of pharmaceutical pollutants from real wastewater samples. *Heliyon* **2019**, *5*, e02339. [CrossRef] [PubMed]

54. Li, Y.; Taggart, M.A.; McKenzie, C.; Zhang, Z.; Lu, Y.; Pap, S.; Gibb, S. Utilizing low-cost natural waste for the removal of pharmaceuticals from water: Mechanisms, isotherms and kinetics at low concentrations. *J. Clean. Prod.* **2019**, *227*, 88–97. [CrossRef]

55. Kumar, S.; Sahu, A.K.; Kumar, M. Heat and water flux modeling in an earth dam. *Water Sci. Technol.* **2021**, *84*, 2760–2779. [CrossRef]